Small molecule inhibitors of transcriptional Cyclin Dependent Kinases impose HIV-1 latency, presenting "block and lock" treatment strategies

Riley M. Horvath[1], Zabrina L. Brumme[2,3], and Ivan Sadowski[1]*

[1]Department of Biochemistry and Molecular Biology
Molecular Epigenetics Group, LSI
University of British Columbia, Vancouver, B.C., Canada

[2]Faculty of Health Sciences
Simon Fraser University, Burnaby, B.C., Canada

[3]British Columbia Centre for Excellence in HIV/AIDS
Vancouver, B.C., Canada

Running Title: Transcriptional CDK inhibitors for Block-and-Lock of HIV-1 provirus

Keywords: CDK7; CDK8; CDK9; CDK19; YKL-5-124; LDC000067; Senexin A; HIV-1; Latency; Transcription; TFIIH; Mediator kinase; P-TEFb; block and lock.

*Correspondence to: I. Sadowski, Dept. of Biochemistry and Molecular Biology, UBC, 2350 Health Sciences Mall, Vancouver, B.C., V6T 1Z3, CANADA; Email: ijs.ubc@gmail.com; Phone: (604) 822-4524; FAX: (604) 822-5227.

Abstract

Antiretroviral therapy is not a cure for HIV-1 infection, as viral rebound inevitably occurs following discontinuation of treatment. The “block and lock” therapeutic strategy seeks to enforce proviral latency and durably suppress viremic reemergence in the absence of other medical intervention. The transcription associated cyclin dependent protein kinases (tCDKs) are required for viral expression from the 5' HIV-1 Long-Terminal Repeat (LTR), but the therapeutic potential of inhibiting these kinases for enforcing HIV-1 latency remains uncharacterized. Here we extended upon previous work to directly compare the effect of highly selective small molecule inhibitors of CDK7 (YKL-5-124), CDK9 (LDC000067), and CDK8/19 (Senexin A), and found each of these prevented HIV-1 provirus expression at concentrations that showed no toxicity. Inhibition of CDK7 caused cell cycle arrest, whereas CDK9 and CDK8/19 inhibitors did not, and could be continuously administered to establish proviral latency. Upon discontinuation of drug administration, HIV immediately rebounded in cells that had been treated with the CDK9 inhibitor, while proviral latency persisted for several days in cells that had been treated with the CDK8/19 inhibitor. Our results identify the mediator kinases CDK8/CDK19 as potential “block and lock” targets for therapeutic suppression of HIV-1 provirus expression.

57 **Introduction**

58 The barrier towards a cure for HIV-1 is the population of extremely long-lived $CD4^+$ T
59 cells that harbor latent provirus. Antiretroviral therapy (ART) is capable of halting disease
60 progression but has no effect on the latent HIV-1 reservoir and consequently, viral replication
61 rapidly rebounds upon discontinuation of treatment (1) (2). The seemingly antithetical proposed
62 "shock and kill" and "block and lock" therapeutic strategies are intended to eliminate the
63 requirement of lifelong ART through manipulation of latent provirus expression (3). The "shock
64 and kill" strategy would involve pharmacological reactivation by latency reversal agents (LRAs)
65 and encouraging destruction of infected cells through viral cytotoxicity and immunological
66 surveillance (4) (5). Development of this strategy faces formidable barriers, as it may be
67 impossible to reactivate the majority of latent provirus (6) (7) (8), and because HIV-1 specific
68 $CD8^+$ lymphocyte-mediated clearance becomes inefficient in individuals on ART (9) (10).
69 Given these limitations, the alternative "block and lock" strategy, by which durable latency is
70 enforced using latency promoting agents (LPAs) to suppress viral rebound in the absence of
71 ART, might represent a more feasible therapeutic option (11) (12). Significant recent attention
72 has been focused on development of these strategies to modulate expression of HIV-1 provirus,
73 and there is the potential that sequential treatment with LRAs and LPAs may contribute to an
74 effective strategy to promote remission. For example, LRAs in combination with other
75 intervention might be first applied to promote killing of as many latently infected cells as
76 possible, which could then be followed with a latency promoting agent to silence the remaining
77 provirus (13).

78 Of the many factors which regulate expression of HIV-1 provirus, the transcription
79 associated cyclin dependent protein kinases (tCDKs) represent important potential targets for

80 latency promoting agents. The RNA Polymerase II associated protein kinases, including CDK7,
81 CDK8, CDK9 and CDK19 are regulated by association with cyclin proteins whose abundance
82 does not fluctuate throughout the cell cycle (14), and function to regulate specific activities of
83 RNA polymerase II (15). Each of the tCDKs play significant roles for regulation of HIV-1
84 provirus expression. Phosphorylation of Serine 5 on the C-terminal domain (CTD) of the largest
85 RNA Polymerase II subunit by CDK7, as part of TFIIH (16) (17), is required for clearance of
86 RNAPII from the core LTR promoter (18), and recruitment of TFIIH to the HIV-1 LTR was
87 shown to be a limiting step for reactivation of HIV-1 provirus expression in response to T cell
88 signaling (19). CDK7 also functions as the CDK-activating kinase for most other CDKs,
89 including those which are directly involved in regulation of cell cycle progression, and
90 consequently CDK7 inhibitors typically have broad effects on transcription and cell growth
91 (20)(21).

92 Like most cellular promoters, RNAPII recruited to the HIV-1 LTR pauses after synthesis
93 of a short nascent leader; the nascent 5' HIV-1 RNA forms the TAR stem loop structure, which
94 binds the viral transactivator protein Tat (22). Tat triggers efficient recruitment of P-TEFb,
95 consisting of CDK9 and Cyclin T1 (23) (24), which phosphorylates Serine 2 of RNAPII in
96 addition to the pausing factors DRB sensitivity-inducing factor (DSIF) and negative elongation
97 factor (NELF) resulting in enhanced transcriptional elongation (25) (26) (27) (28). In addition to
98 Tat, the host co-activator TRIM24 was shown to promote recruitment of CDK9 to the HIV-1
99 LTR to stimulate elongation (29) (30). CDK9 inhibitors, including purine derivatives
100 (Roscovitine) and flavonoids (flavopiridol), repress HIV-1 expression (31) (32) (33). However,
101 these drugs lack specific activity against CDK9 as they also inhibit CDK2, CDK5, and CDK7, in

102 addition to other cellular enzymes (34) (33), an effect that causes global inactivation of RNAPII
103 and cell cycle arrest (35) (36).

104 The mediator kinase module, consisting of Cyclin C, MED12, MED13, and CDK8 or its
105 paralog CDK19, transiently associates with the core mediator complex at the promoter of signal-
106 responsive genes and selectively regulates transcription by phosphorylating transcription factors
107 (37) (38). CDK8/19 kinase activity can produce both positive and negative effects on
108 transcription, depending on the functional effect of the modification (37) (39) (40). We recently
109 demonstrated that specific chemical inhibitors of CDK8/19 or *CDK8* gene knockout inhibit
110 reactivation of HIV-1 provirus (41), an outcome that is possibly mediated by the effects of
111 CDK8/19 on transcriptional activators that bind the LTR enhancer such as NFκB (42), TCF/LEF
112 β-catenin (43), and STAT1/3 (44). These observations indicate that CDK8/19 inhibitors could be
113 used for block and lock therapies, but the potential of such compounds for this purpose have not
114 been examined.

115 Inhibitors of tCDK activity, particularly of CDK9 (45) (46), have been suggested as
116 potential "block and lock" reagents (12), but the effectiveness of specific inhibitors of CDK7,
117 CDK9, and CDK8/19 for this purpose has not been established. Recently, more highly specific
118 small molecule inhibitors of CDK7 and CDK9 have been developed (47) (48), and this
119 technological advancement enabled direct comparison of effects caused by specific inhibitors of
120 these kinases on HIV-1 provirus expression, which we describe in this report. We compared the
121 effect of inhibitors of CDK7 (YKL-5-124) (47), CDK9 (LDC000067) (48), and CDK8/19
122 (Senexin A) (49) on HIV-1 provirus expression. Each of these compounds inhibited HIV-1
123 provirus expression in model T cell lines and primary $CD4^+$ peripheral blood mononuclear cells
124 (PBMCs) isolated from people living with HIV-1. Treatment of cells with CDK9 and CDK8/19

125 inhibitors was well tolerated over long durations of exposure, whereas CDK7 inhibition caused
126 cell cycle arrest and reduced cell viability. Long term treatment of HIV-1 infected cells with
127 LDC000067 and/or Senexin A established drug induced latency. Interestingly, upon removal of
128 drug we found that latency persisted in cells that had been treated with the CDK8/19 inhibitor
129 Senexin A, while immediate HIV-1 rebound occurred in cells previously treated with the CDK9
130 inhibitor LDC000067. This indicates that prolonged inhibition of CDK8/19 may produce an
131 epigenetic state on the HIV-1 LTR promoter that is reticent to stochastic reactivation. Overall,
132 these observations present CDK8/19 as a significant potential target for "block and lock"
133 strategies to produce durable HIV-1 proviral latency.

Results

tCDK activity is required for HIV-1 induction in response to T cell activation. We examined the requirement of tCDK activity for HIV-1 expression using the specific small molecule inhibitors YKL-5-124 (CDK7i), LDC000067 (CDK9i), and Senexin A (CDK8/19i) (Fig. 1*A*-*C*). These recently developed chemical inhibitors display vastly improved target selectivity over previously described CDK inhibitors (47)(48)(49). We assessed the effect of these compounds on cell viability, determining half lethal concentration (LC50) of 93 μM, 499 μM, and 200 μM for YKL-5-124 (CDK7i), LDC000067 (CDK9i), and Senexin A (CDK8/19i), respectively (Fig. 1*D*). We then examined the effects of these drugs at non-toxic concentrations on expression of HIV-1 provirus using the well-described JLat10.6 and JLat9.2 models of HIV-1 latency. Derived from the Jurkat human T-cell line, JLat cells possess a full-length replication (envelope)-defective provirus where *Nef* was replaced with GFP, such that GFP expression is dependent upon transcriptional activity of the 5' HIV-1 LTR (50). Treatment with YKL-5-124, LDC000067, or Senexin A caused dose-dependent inhibition of HIV-1 induction in response to PMA/ionomycin in the JLat10.6 cell line (Fig. 2*A*-*C*). When calculated as the percentage of cells expressing GFP, we found that YKL-5-124 (CDK7i) was the most potent, with a half inhibitory concentration (IC50) for GFP expression of 0.11 μM, while LDC000067 and Senexin A produced IC50 values of 1.42 μM and 15.43 μM, respectively (Fig. 2*B*). Comparable results were observed when GFP Mean Fluorescence Intensity (MFI) was used as a readout (Fig. 2*C*). A similar inhibitory effect was observed with the JLat9.2 cell line (Fig. 2*D*), although lower concentrations of inhibitor suppressed proviral expression (Fig. 2*E*, 2*F*). Again, the CDK7i YKL-5-124 was the most potent (IC50: 0.02 μM), while LDC000067 and Senexin A had IC50 values of 0.56 μM and 0.43 μM, respectively. Notably, viability of JLat10.6 and JLat9.2 cells

were not affected by the tCDK inhibitors at concentrations that impair HIV-1 expression (Fig. S1).

The JLat10.6 and JLat9.2 cell lines, typical of other cell lines bearing HIV-1 reporter provirus (51), produce distinct patterns of GFP reporter expression in response to T cell activation, where ~70% of JLat10.6 and ~14% of JLat9.2 cells fully express GFP upon treatment with PMA and ionomycin, while the rest of cells in the populations remain uninduced (Fig. 2*A*, 2*D*, Vehicle). Treatment of PMA/ ionomycin stimulated cells with LDC000067 (CDK9i) or Senexin A (CDK8/19i) diminished the proportion of GFP+ cells (Fig. 2*B*, 2*E*), but caused a similar bimodal distribution of GFP expression, where provirus that escape latency in response to simulation induce full GFP expression (Fig. 2*A*, 2*D*, LDC000067, Senexin A). In contrast, treatment with the CDK7 inhibitor YKL-5-124 produces a larger gradient of GFP expression in PMA/ ionomycin stimulated cells, particularly in the JLat10.6 cell line, where a significant proportion of stimulated cells express lower levels of GFP (Fig. 2*A*, 2*D*, YKL-5-124). These differences in GFP expression patterns in stimulated cells may reflect the distinct effects these inhibitors have on RNAPII activity.

tCDK inhibitors have synergistic effects on HIV-1 expression. CDK7, CDK9, and CDK8/19 regulate different aspects of RNAPII function, and consequently we expected that combined treatment with inhibitors specific for tCDKs would produce synergistic effects for inhibition of HIV-1 provirus expression. To examine this possibility, we treated JLat10.6 cells with YKL-5-124 (CDK7i) and LDC000067 (CDK9i) (Fig. 3*A*), YKL-5-124 (CDK7i) and Senexin A (CDK8/19i) (Fig. 3*B*), or LDC000067 (CDK9i) and Senexin A (CDK8/19i) (Fig. 3*C*), at suboptimal inhibitory concentrations for each, and induced provirus expression by stimulation with PMA and ionomycin. In this analysis we found that co-treatment with any pair of tCDK

180 inhibitors produced a greater inhibitory effect on HIV-1 expression than individual treatment
181 with the inhibitors (Fig. 3*A*-*C*) indicating these effects were synergistic, as determined by ΔFa_{xy}
182 values >0 as calculated using Bliss independence modelling (52)(53)(54). Among these
183 combinations we found that LDC000067 (CDK9i) and Senexin A (CDK8/19i) produced the
184 greatest synergistic inhibition of HIV-1 reactivation (Fig. 3*D*-*F*). The synergistic inhibitory
185 effect for all combinations was most pronounced at lower drug concentrations, and decreased at
186 the highest concentrations, where GFP expression was minimal (Fig. 3*D*-*F*). These observations
187 indicate selectivity of the tCDK inhibitors for CDK7, CDK9, or CDK8/19, and suggest that these
188 kinases function through independent mechanisms for regulation of RNAPII. Importantly, cell
189 viability was not affected at inhibitor concentrations where we observed synergistic inhibitory
190 effects on HIV-1 provirus expression (Fig. S2).

191 ***tCDK inhibitors antagonize proviral reactivation in response to mechanistically diverse***
192 ***latency reversal agents.*** Having observed that tCDK inhibition suppresses reactivation of latent
193 provirus in response to T cell activation, we next examined their effects on a variety of
194 mechanistically diverse latency reversal agents (LRAs). As mentioned above, co-treatment with
195 the phorbol ester PMA and the ionophore ionomycin triggers T cell activation by stimulating
196 Ras-MAPK, PKC-NFκB, and calineurin-NFAT (55). Ingenol 3-angelate (PEP005) activates
197 PKC- NFκB, partially mimicking T cell activation (56). JQ1 and IACS-9571 are bromodomain
198 inhibitors that reverse latency by interfering with function of their respective targets, BRD4 (57)
199 and TRIM24 (29). Finally, suberanilohydroxamic acid (SAHA) is a well-studied histone
200 deacetylase inhibitor (HDACi) known to reactivate HIV-1 expression *in vitro* and *in vivo*
201 (58)(59). Of these LRAs, the bromodomain inhibitors JQ1 and IACS-9571 induced only modest
202 proviral reactivation in the JLat10.6 cell line (Fig. 4*A*, 4*B*, black bar). In contrast,

203 PMA/ionomycin, the NFκB agonist PEP005, alone or in combination with IACS-9571 and the
204 HDACi SAHA produced markedly higher levels of HIV-1 provirus expression (Fig. 4*A*, 4*B*).

205 To examine the effect of tCDK inhibitors on reactivation by these LRAs, we co-treated
206 cells with concentrations of tCDK near the IC50 for inhibition of PMA/ionomycin induced
207 expression in JLat10.6 cells, which was 100 nM YKL-5-124 (CDK7i), 1 μM LDC000067
208 (CDK9i), or 10 μM Senexin A (CDK8/19i). CDK7 inhibition by YKL-5-124 limited proviral
209 reactivation, as measured by the proportion of GFP+ cells, in response to every LRA other than
210 JQ1 where oddly, we observed an increased proportion of GFP expressing cells (Fig. 4*A*).
211 Interestingly, although inhibition of CDK7 produced a greater proportion of GFP+ cells when
212 treated with JQ1 (Fig. 4*A*), the GFP MFI value was decreased compared to the vehicle control
213 (Fig. 4*B*) indicating that more cells expressed GFP but at attenuated levels in the presence of
214 YKL-5-124. Treatment with LDC000067 (CDK9i) or Senexin A (CDK8/19i) inhibited
215 reactivation of HIV-1 in response to all LRAs (Fig. 4*A*, 4*B*). Consistent with previous
216 observations (29), we observed a synergistic effect for HIV-1 reactivation by co-treatment with
217 the NFκB agonist PEP005 and the TRIM24 bromodomain inhibitor IACS-9571 (Fig. S3).
218 Moreover, tCDK inhibitors were the least effective at preventing reactivation of provirus in cells
219 treated with the combination of PEP005 and IACS-9571 (Fig. 4*A*, 4*B*). Finally, although the
220 tCDK inhibitors suppressed appearance of GFP positive cells in response to PMA/ ionomycin
221 treatment by approximately equivalent amounts (Fig. 4*A*, PMA/Ionomycin), certain inhibitors
222 were more effective at inhibiting reactivation by particular LRAs. For instance, Senexin A
223 (CDK8/19i) was most effective at suppressing SAHA mediated activation (Fig. 4*A*, SAHA)
224 while LDC000067 (CDK9i) was most potent at inhibiting expression in response to JQ1 (Fig.

4*A*, JQ1). Taken together, these results indicate that tCDK inhibition suppresses proviral activation in response to mechanistically diverse latency reversing agents.

Requirement of Tat for the effect of tCDKs on HIV-1 transcription. We then examined the dependence of CDK7, CDK9, and CDK8/19 on the viral transactivator Tat for activation of HIV-1 transcription. The Jurkat derived JLatA72 cell line possesses an integrated HIV-1 LTR that drives expression of GFP but unlike the JLat10.6 and JLat9.2 cell lines, does not express the viral transactivator Tat (60). Untreated JLatA72 cells express GFP in ~30% of the population, and this proportion increases to ~60% upon treatment with PMA/ionomycin (Fig. 5*A*, 5*B*, Unstimulated, Vehicle). To examine the effect of tCDK inhibitors on HIV-1 expression in the absence of Tat, we treated JLatA72 cells with the kinase inhibitors and subsequently induced T cell activation with PMA/ionomycin. Surprisingly, we found that inhibition of CDK7 with YKL-5-124 caused an increase in the proportion of GFP positive cells in stimulated cells (Fig. 5*A*, 5*B*) while also lowering overall proviral expression in these cells (Fig. 5*C*), an effect that is similar to that described above for co-treatment with JQ1 (Fig. 4). The CDK9 inhibitor LDC000067 had no effect on the proportion of GFP positive cells (Fig. 5*A*, 5*B*) and only slightly decreased overall GFP expression (Fig. 5*C*), consistent with the role of Tat for recruitment of CDK9 to the HIV-1 LTR. Inhibition of CDK8/19 with Senexin A decreased both the proportion of cells expressing GFP in response to PMA/ionomycin (Fig. 5*A*, 5*B*), and suppressed overall levels of GFP expression in induced cells (Fig. 5*C*), indicating that the effect of CDK8/19 on reactivation of HIV-1 expression is not solely dependent on Tat.

We also examined the effect of tCDK inhibitors in the CEM derived GXR-5 cell line, which like JLatA72, possess a chromosomally integrated HIV-1 LTR GFP reporter that does not express Tat (61). However, unlike JLatA72 cells, GXR-5 cells produce a basal level of provirus

expression such that most untreated cells express some amount of GFP (Fig. S4*A*, Fig. S4*B*). However, stimulation with PMA/ionomycin causes an increase in GFP+ expression as measured by Mean Fluorescence Intensity (MFI) (Fig. S4*C*). Similar to results with the JLatA72 cell line, GXR-5 cells produced significantly attenuated induction of GFP induction upon treatment with YKL-5-124 (CDK7i) or Senexin A (CDK/19i) (Fig. S4*C*). In contrast, LDC000067 (CDK9i) caused a small but significant inhibition of GFP expression (Fig. S4*C*), which supports the requirement of CDK9 for Tat function.

Effect of tCDK inhibition on cell growth. The results presented above indicate that tCDK activity is necessary for reactivation of HIV-1 provirus. Given the stochastic expression phenotype observed for latent provirus (51) (62) (63), therapies intended to prevent HIV-1 reactivation will likely necessitate prolonged treatment to produce latency that could persist subsequent to drug withdrawal. To further examine the cellular impact of tCDK inhibition, we examined growth and viability of Jurkat T cells exposed to a range of tCDK inhibitor concentrations for 4 -days. This revealed concentrations of YKL-5-124 (CDK7i) that inhibited HIV-1 provirus expression, completely prevented cell growth and caused cell cycle arrest (Fig. 6*A*), a result that is consistent with the defined function of CDK7 as the CDK-activating kinase (CAK) which phosphorylates and activates CDKs that have essential roles for cell-cycle progression (64). Moreover, treatment with YKL-5-124 causes toxicity that becomes apparent after 3 or -4 days of treatment, depending on the concentration (Fig. 6*B*). In contrast, the CDK9 inhibitor LDC000067 and CDK8/19 inhibitor Senexin A caused minimal effects on cell growth (Fig. 6*C, E*) and cell viability (Fig. 6*D, F*) at concentrations that limit HIV-1 provirus expression, athough cell growth was prevented (and in the case of LDC000067, also induced toxicity) at

higher concentrations. These observations indicate that long-term inhibition of CDK9 and/or CDK8/19, but not CDK7, may be tolerated for suppression of HIV-1 provirus reactivation.

Role of tCDKs for the establishment of immediate latency. Upon infection of T cells with HIV-1, nearly 50% of newly integrated provirus become transcriptionally repressed within 48 hours post-infection, despite the site of chromosomal integration, a phenomenon known as immediate latency (65, 66) (67). Because the tCDKs are required for reactivation of HIV-1 in response to various LRAs and T cell signaling agonists, we also examined the effect of these inhibitors on outcome of initial infection by HIV-1. For this analysis we used the Red-Green-HIV-1 (RGH) dual-reporter virus (Fig. 7*A*) (65)(66), which expresses GFP from the 5' LTR and mCherry from an internal promoter, and which produces all of the HIV-1 gene products, apart from *env* and *nef* (66). Upon infection with this reporter virus, cells expressing mCherry from the PGK promoter, but do not express GFP from the 5' HIV-1 LTR represent latently infected cells, while those that express both mCherry and GFP are productively infected (65)(66). To assess the role of tCDK activity on establishment of immediate latency, we pre-treated Jurkat $CD4^+$ T cells with the kinase inhibitors and subsequently infected with RGH at a low multiplicity of infection (MOI). One day post-infection, the cells were either washed to remove residual drug or were maintained in media with the kinase inhibitors, and proviral expression was assessed 4 days post-infection by flow cytometry (Fig. 7*B*, 7*C*). Inhibition of either CDK7 with YKL-5-124 or CDK8/19 with Senexin A at the time of infection reduced the proportion of productively infected cells 4 days later, whereas inhibition of CDK9 with LDC000067 had no effect (Fig. 7*D*, Washed), indicating that CDK9 and Tat are not involved in the decision to formulate latency at the point of infection. Consistent with the results shown above indicating that tCDK inhibition prevents reactivation of latent provirus (Fig. 2, Fig. 4), maintained treatment with the kinase inhibitors post-infection

293 decreased the proportion of productively infected cells, indicating these drugs encourage latency
294 (Fig. 7*D*, Maintained).

295 Surprisingly, we found that inhibition of CDK7 with YKL-5-124 caused approximately
296 double the rate of infection, indicating that loss of CDK7 activity may render T cells susceptible
297 to infection (Fig. 7*E*). Notably, although CDK7 inhibition caused an increase in the proportion
298 of HIV-1 infected cells (Fig 7*E*), the infected population is enriched for latent provirus, as just
299 over 20% were productively infected (Fig. 7*C*, 7*D*, compare Untreated to YKL-5-124).
300 Importantly, kinase inhibition did not affect cellular viability (Fig. S5). These results reveal that
301 the inhibition of CDK7 or CDK8/19 at the point of infection inhibits formation of productive
302 infection after removal of the drug, inhibition of CDK9 does not have this lasting effect.
303 Although the CDK7 inhibitor YKL-5-124 has this latency promoting affect in newly infected
304 cells, it has associated shortcomings of inducing cell cycle arrest (Fig. 6*A*) and rendering cells
305 susceptible to infection (Fig. 7*E*).

306 ***Inhibition of CDK8/19 but not CDK9 induces durable latency.*** An optimal "block and lock"
307 therapy would involve treatment(s) that induce durable latency, even after the latency promoting
308 agent (LPA) is removed. To examine the capability of the tCDK inhibitors to induce durable
309 latency, we examined the effect of these compounds on the mdHIV #77 cell line (51), which is
310 derived from Jurkat Tat cells and bears a replication incompetent mini-dual reporter HIV-1
311 provirus that is integrated into an intron of the *PACS1* gene in the (+) orientation (Fig. 8*A*). HIV-
312 1 reporter cell lines typically produce stochastic bursts of HIV-1 expression (51)(62), and
313 consistently ~3% of untreated mdHIV #77 cells co-express dsRed from the 5' HIV-1 LTR and
314 eGFP from an internal EF1α promoter (Fig. 8*C*, Vehicle) (51). To examine the effect of tCDK
315 inhibitors on stochastic expression of latent HIV-1 provirus we treated mdHIV #77 cells for 14

316 days with the tCDKi, after which the drugs were removed by washing the cells. Expression of
317 dsRed from the 5' HIV-1 LTR was monitored for 10 days following removal of the drugs by
318 flow cytometry (Fig. 8*B*, 8*C*). The effect of the CDK7 inhibitor YKL-5-124 (CDK7i) in this
319 experiment was not assessed because of associated toxicity (Fig. 6*A*, 6*B*).

320 We observed that stochastic HIV-1 expression was suppressed in this cell line by
321 treatment with LDC000067 (CDK9i) and/or Senexin A (CDK8/19i) following 4 days of
322 treatment (Fig. 8*C*, 8*D*). Following removal of the CDK inhibitors, we found that cells that had
323 been treated with LDC000067 (CDK9i) produced an immediate rebound of provirus expression,
324 as the population of dsRed+/eGFP+ cells nearly matched that of untreated cells within 24 hrs of
325 drug withdrawal (Fig. 8*D*, compare day 14 to 15). In contrast, mdHIV #77 cells that had been
326 treated with Senexin A (CDK8/19i) alone, or in combination with LDC000067 (CDK9i),
327 maintained decreased levels of dsRed expression for 10 days following drug removal (Fig. 8*D*,
328 Drug Removed). Importantly, none of the inhibitors affected cell viability over the course of
329 treatment (Fig. 8*E*). We observed similar results with the Jurkat Tat mdHIV #110 clonal line
330 (Fig. S6). This line has the mini-dual HIV-1 reporter integrated in the (-) orientation in the
331 *BTBD10* gene, and produces stochastic dsRed expression in ~25% of untreated cells (51) (Fig.
332 S6*C*, Vehicle). Treatment of mdHIV #110 cells with the CDK9 and CDK8/19 inhibitors
333 suppressed HIV-1 LTR dsRed expression (Fig. S6*D*, Drug Treated). But removal of drug from
334 cells treated with LDC000067 (CDK9i) resulted in immediate rebound of dsRed expression,
335 whereas dsRed expression gradually increased over the week following removal of drug(s) from
336 cells treated with Senexin A (CDK8/19i), alone or in combination with LDC000067 (Fig. S6*D*,
337 Drug Removed). Again, we did not observe effects on viability of mdHIV #110 cells over the
338 course of tCDKi treatment (Fig. S6*E*).

Cell lines bearing the mdHIV reporters constitutively express Tat protein, but this provirus does not express any other viral gene products. To examine the effect of the tCDK inhibitors on HIV-1 provirus in more detail, we produced a clonal Jurkat T cell line bearing an integrated RGH reporter virus, which encodes all of the viral genes, apart from *env* and *nef,* and where Tat expression is dependent upon normal expression from a subgenomic HIV-1 transcript (Fig 9A, RGH #20). These cells were treated for 7 days with LDC000067 (CDK9i) and/or Senexin A (CDK8/19i), at which point the cells were washed and GFP expression was monitored for 10 days following drug removal (Fig. 9*B*). Treatment of RGH #20 cells with the tCDK inhibitors suppressed provirus expression within 4 days (Fig. 9*C*, 9*D*, Drug Treated). Consistent with the results described above with the mdHIV cell lines, we found that removal of drug from RGH #20 cells treated with the CDK9 inhibitor LDC000067 resulted in immediate rebound of LTR driven GFP expression, indicating reactivation of basal HIV-1 transcription. In contrast, in cells treated with the CDK8/19 inhibitor Senexin A, alone or in combination with LDC000067, we observed suppression of HIV-1 GFP expression for four days following removal of the drug(s), and full rebound of expression was not observed until 10 days later (Fig. 9*D*, Drug Removed). As with the experiments described above, we did not observe effects on cell viability in treatment of the RGH #20 cell line (Fig. 9*E*). These results suggest that CDK8/19 inhibitors, but not inhibitors of CDK9, induce a repressive configuration of the HIV-1 promoter that persists following removal of treatment.

tCDK inhibitors suppress proviral expression in cells from people living with HIV-1 ex vivo. To directly compare effectiveness of tCDK inhibitors on HIV-1 provirus expression, we examined the effect of these compounds on reactivation of provirus in primary peripheral blood mononuclear cells (PBMCs) isolated from individuals living with HIV-1 and receiving

362 suppressive antiretroviral therapy (Table 1). In cells from these individuals, we observed
363 increased HIV-1 mRNA in response to PMA/ionomycin treatment (Fig. 10, compare
364 Unstimulated to Vehicle). Consistent with the above results, treatment with YKL-5-124
365 (CDK7i) decreased provirus expression in all three participants, while treatment with
366 LDC000067 (CDK9i) or Senexin A (CDK8/19i) decreased provirus expression in two of three
367 participants (Fig. 10). Interestingly, the combination of LDC000067 and Senexin A produced
368 the most robust silencing of viral expression in all three participants (Fig. 10,
369 LDC000067/Senexin A), with Participant A displaying even lower expression of HIV-1 mRNA
370 than when left unstimulated (Fig. 10*A*). Furthermore, for Participant C we observed synergistic
371 inhibition of expression with LDC000067 and Senexin A co-treatment (Fig. 10*C*). These results
372 indicate that tCDK inhibition can suppress proviral reactivation in cells from individuals living
373 with HIV *ex vivo*.

374 **Discussion**

375 Development of therapeutic strategies to eliminate the life-long requirement of ART for
376 people living with HIV-1 are currently aimed at modulating expression of the latent provirus (3).
377 The proposed "shock and kill" strategy for elimination of latently infected cells has been one
378 focus of intense investigation, and although a variety of latency reversing agents have been
379 identified (68)(6), none have successfully reduced the latent population in infected individuals
380 (69), largely because of an inefficient anti-HIV-1 cellular immune response (4) (70)(69, 71).
381 The antithetical "block and lock" strategy may be a more feasible approach towards treatment of
382 the latently infected population for functional elimination of HIV-1, and this contention is
383 supported by results shown here. Block and lock would involve use of latency promoting agents
384 (LPAs) to suppress stochastic expression of viral transcripts from the 5' LTR, which may lead to
385 sustained epigenetic silencing of integrated provirus (11) (12). Although several LPAs such
386 as didehydro-cortistatin A (dCA) (72) (73) and spironolactone (74) have displayed promising
387 results *in vitro*, no human trials with latency enforcing compounds have been performed. In the
388 present study, we directly compared the transcriptional Cyclin Dependent Kinases (tCDKs)
389 CDK7, CDK9, and CDK8/19 as potential targets for enforcement of proviral latency in various
390 cell line models as well as primary PBMCs isolated from people living with HIV-1. Our results
391 indicate that CDK8/19 inhibitors in particular, could contribute to implementation of this
392 strategy.

393 Recruitment of the general transcription factor TFIIH to the LTR is rate limiting for
394 reactivation of latent HIV-1 (19). The TFIIH complex is composed of 10 proteins consisting of a
395 core component (XPB, XPD, p62, p52, p44, p34, p8) and a CDK-activating kinase (CAK)
396 module (CDK7, cyclin H, MAT1) (75). Consistent with the requirement of TFIIH for

397 reactivation of viral transcription, we found that treatment with the selective CDK7 inhibitor
398 YKL-5-124 prevented induction of HIV-1 in response to T cell activation (Fig. 2). Furthermore,
399 YKL-5-124 was found to limit proviral reactivation in response to several diverse LRAs,
400 including the TRIM24 bromodomain inhibitor IACS-9571 and the HDACi SAHA (Fig. 4).
401 Surprisingly, inhibition of CDK7 in combination with JQ1 caused an increased proportion of
402 cells possessing productive HIV-1 (Fig. 4*A*), although viral expression was severely diminished
403 in these cells (Fig. 4*B*). Interestingly, we observed a similar effect when we examined
404 reactivation of HIV-1 provirus in JLatA72 cells treated with YKL-5-124 (Fig. 5). These
405 observations might also be related to our finding that inhibition of CDK7 is associated with
406 increased susceptibility of T cells for HIV-1 infection (Fig. 7). TFIIH has both helicase and
407 protein kinase activities that facilitate promoter opening and catalyze phosphorylation of
408 RNAPII CTD S5 (74) (19). Our peculiar finding that inhibition of CDK7 causes an increased
409 proportion of cells to become infected by HIV-1, albeit being enriched for latent provirus, likely
410 represents a function of TFIIH for HIV-1 transcription that has not been characterized. We
411 found that inhibition of HIV-1 expression by the CDK7 inhibitor YKL-5-124 only occurred at
412 concentrations that caused significant inhibition of cell cycle progression (Fig. 6*A*, 6*B*), which
413 suggests that inhibitors of CDK7 may not be appropriate for therapeutic use. The latency
414 promoting agent spironolactone causes proteasomal degradation of the XBP subunit of TFIIH
415 and was shown to enforce HIV-1 latency, but viral rebound in cells treated with this drug
416 occurred immediately upon withdrawal (74). Furthermore, although spironolactone causes
417 efficient reduction in XPB protein levels, it also causes reduced expression of CDK7 (74),
418 indicating this potential LPA may also have cytotoxic effects.

419 The transcriptional elongation factor P-TEFb, comprised of Cyclin T1 and CDK9, is
420 recruited to the nascent HIV-1 LTR TAR RNA through interaction with Tat, and facilitates
421 escape of promoter proximal paused RNAPII, which produces a strong positive feedback loop
422 for HIV-1 provirus expression (76). Consistent with this defined function of CDK9, we found
423 that a selective inhibitor of CDK9 kinase activity, LDC000067 (48), suppressed HIV-1 proviral
424 induction in multiple HIV-1 provirus reporter cell lines (Fig. 2, Fig. 4), and in PBMCs from
425 people living with HIV-1 *ex vivo* (Fig. 10). We also confirmed that the function of CDK9 for
426 HIV-1 expression is largely dependent upon the viral transactivator Tat, as LDC000067 had no
427 appreciable effect in in JLatA72 cells, which do not express Tat (Fig. 5, Fig. S4). Given the
428 predominant role of CDK9 for HIV-1 transcription, this enzyme is an important potential
429 therapeutic target (77) (78) and previous results have shown the CDK9 inhibitors Roscovitine,
430 flavopiridol, and seliciclib to supress HIV-1 replication (31)(32)(79)(33). However, these
431 previously characterized compounds are properly described as pan-CDK inhibitors as they are
432 not selective and cause global inactivation of RNAPII transcription and cell cycle arrest (35)(36).

433 Importantly, in the present study we found that the selective CDK9 inhibitor LDC000067
434 had no effect on cell growth or viability at concentrations effective at restricting proviral
435 expression (Fig. 6*C*, 6*D*). Consequently, we were able to assess the capability of CDK9
436 inhibition to generate durable latency. In all T cell models examined, LDC000067 treatment
437 generated proviral latency without affecting cell growth (Fig. 8, Fig. 9, Fig. S6, see Drug
438 Treated). However, removal of the CDK9 inhibitor from treated cells corresponded with
439 immediate rebound of HIV-1 stochastic basal expression to levels seen in untreated cells (Fig. 8,
440 Fig. 9, Fig. S6, see Drug Removed). There is significant interest in disrupting the Tat-CDK9
441 positive feedback loop for effective "block and lock" therapies, and various strategies for

442 inhibition of Tat have been proposed, including forcing its degradation by the long noncoding
443 RNA NRON (80) and expression of the Tat mutant designated Nullbasic (81) (82). Given that
444 the role of Tat for HIV-1 replication involves recruitment of P-TEFb (CDK9/Cyclin T1) to the 5'
445 LTR and that we observed that CDK9 inhibition did not generate lasting latency, our results
446 indicate that sole disruption of the positive feedback loop for expression of HIV-1 provirus is
447 incapable of manifesting durable latency.

448 We recently demonstrated that inhibition of CDK8 restricts HIV-1 provirus expression
449 (41). In this report we show that the CDK8/19 inhibitor suppresses viral induction in response to
450 a diverse set of LRAs and T cell activation (Fig. 2, Fig. 4). Unlike CDK9, the function of
451 CDK8/19 for HIV-1 expression is not dependent on Tat (Fig 5, Fig. S4), consistent with previous
452 findings that CDK8/19 inhibition limits reactivation of ACH2 and U1 proviral latency cell
453 models (41). We observed synergistic inhibition of HIV-1 provirus expression in cells treated
454 with the CDK8/19 inhibitor Senexin A in combination with inhibitors of either CDK7 or CDK9,
455 consistent with the defined role of these kinases for regulating distinct functions for RNAPII
456 transcription. Intriguingly, we found that inhibition of CDK8/19 in multiple cell lines bearing
457 HIV-1 reporter virus caused suppression of stochastic HIV-1 expression, an effect that persisted
458 upon removal of the kinase inhibitor. CDK8/19 inhibition at the time of infection was sufficient
459 to cause a significant decrease in the proportion of transcriptionally active provirus in the days
460 that followed (Fig. 7). Furthermore, inhibition of CDK8/19 with Senexin A generated HIV-1
461 latency that was maintained for days following removal of the drug (Fig. 8, Fig. 9, Fig. S6).
462 These results suggest that inhibition of CDK8/19 causes modification of transcription factors,
463 and/ or chromatin organization associated with HIV-1 provirus that persists following removal of
464 the inhibitor.

465 In this study, we have evaluated the therapeutic potential of targeting the transcription
466 associated protein kinases CDK7, CDK9, and/or CDK8/19 as potential targets for HIV-1
467 therapies. We found that CDK7 inhibition caused cellular toxicity but also increased
468 susceptibility HIV-1 infection in cell lines. Although the CDK9 inhibitor LDC000067 was well
469 tolerated and caused suppression of proviral expression, treatment with this inhibitor did not
470 cause durable latency upon removal of treatment. In contrast we found that the CDK8/19
471 inhibitor Senexin A restricted HIV-1 expression at concentrations that did not affect cellular
472 growth, which also promoted HIV-1 latency, an effect that was maintained for multiple days
473 following drug withdrawal. These results indicate inhibition of CDK8/19 causes persistent HIV-
474 1 provirus latency, an effect that could be exploited with synergistic latency promoting agents to
475 maintain suppression of HIV-1 provirus expression following discontinuation of ART.

Materials and Methods

Cell culture, virus culture, and lentiviral transduction

Jurkat E6-1, Jurkat Tat mHIV-Luciferase, JLat10.6, JLat9.2, JLatA72, and GXR-5 CEM cells were cultured in Roswell Park Memorial Institute 1640 (RPMI-1640) medium supplemented with 10% FBS, penicillin [100 units/ml], streptomycin [100 g/ml], and L-glutamine [2 mM]. HEK293T cells were cultured in Dulbecco's modified Eagle's (DMEM) medium supplemented with 10% fetal bovine serum (FBS), penicillin [100 units/ml], streptomycin [100 g/ml], and L-glutamine [2 mM]). All cell lines were incubated in a humidified 37°C and 5% CO_2 atmosphere.

Peripheral Blood Mononuclear Cells (PBMC) from participants with HIV-1 on ART were isolated from whole blood by density gradient centrifugation using Lymphoprep™ and SepMate™ tubes (StemCell Technologies), and cryopreserved. Upon thawing, PBMCs were cultured in RPMI supplemented with 10% FBS, penicillin [100 units/ml], streptomycin [100 g/ml], and L-glutamine [2 mM]. Samples from participants were collected with written informed consent under a protocol jointly approved by the research ethics boards at Providence Health Care/UBC and Simon Fraser University (certificate H16-02474).

Vesicular stomatitis virus G (VSV-G) pseudotyped viral stocks were produced by co-transfecting HEK293T cells with a combination of viral molecular clone, psPAX, and VSV-G at a ratio of 8 μg : 4 μg : 2 μg. Transfections were performed with polyethylenimine (PEI) at a ratio of 6:1 (PEI:DNA) in Gibco Opti-MEM^{tm}. Lentiviral infections were performed by plating $1x10^6$ cells in 24-well plates with media containing 8 μg/mL polybrene and the amount of viral

supernatant to give the desired multiplicity of infection (M.O.I.) as indicated. Plates were subsequently spinoculated for 1.5 hrs at 1500 rpm.

RT-PCR

RNA was extracted from cells using the RNeasy Kit (Qiagen) and analyzed with the Quant Studio 3 Real-Time PCR system (Applied Biosystems) using *Power* SYBR® Green RNA-to-CT™ 1-Step Kit (Thermo Fisher) as per the manufacturer's instructions. RT-PCR data was normalized to GAPDH expression using the ΔΔCt method as previously described (Livak & Schmittgen, 2001). Cycling parameters were as follows: 48 ^{o}C, 30 min, 1x; 95 ^{o}C, 10 min, 1x; (95 ^{o}C, 15 sec, 60 ^{o}C, 1 min), 60x. Primers were as follows: HIV-1 mRNA (multiply spliced Tat-Rev transcripts), Fwd 5' CTTAGGCATCTCCTATGGCAGGA, Rev 5' GGATCTGTCTCTGTCTCTCTCTCCACC; GAPDH, Fwd 5' TGCACCACCAACTGCTTAGC, Rev 5' GGCATGGACTGTGGTCATGAG.

Flow cytometry

Cells were treated as indicated in the figure legends. Human T cell lines were suspended in PBS and a BD Biosciences LSRII-561 system was used for flow cytometry with threshold forward scatter (FSC) and side scatter (SSC) parameters being set so that a homogenous population of live cells was counted. FlowJo software (TreeStar) was used to analyze data and determine the indicated Mean Fluorescence Intensity (MFI).

Quantitative analysis of tCDK inhibitor latency promoting agent interaction

Bliss independence modeling was used as previously described (29) to statistically assess the inhibitory activity of combinatorial tCDK inhibitor treatment on HIV-1 reactivation. The equation $Fa_{xy,\,P} = Fa_x + Fa_y - (Fa_x)(Fa_y)$ defines the Bliss independence model, in which $Fa_{xy,}$

$_P$ is the predicted fraction affected by a combination of drug *x* and drug *y* that is derived from the experimentally observed fraction affected by drug *x* (Fa_x) and drug *y* (Fa_y) individually. Comparison of the predicted combinatorial affect ($Fa_{xy,P}$) with the experimentally observed impact ($Fa_{xy,O}$) was then performed: $\Delta Fa_{xy} = Fa_{xy,O} - Fa_{xy,P}$. If ΔFa_{xy} is greater than 0, the combination of drugs *x* and *y* exceed that of the predicted affect indicating that the drugs display synergistic interaction. If $\Delta Fa_{xy} = 0$, the drug combination follows the Bliss model for independent action. If ΔFa_{xy} is less than 0, the drug interaction is antagonistic as the observed effect of the drug combination is less than predicted.

Statistics and reproducibility

All replicates are independent biological replicates and are presented as mean values with ± standard deviation shown by error bars. The number of times that an experiment was performed is indicated in the figure legends. P-values were determined using unpaired *t*-tests using GraphPad Prism 9.0.0. Statistical significance is indicated at $*P < 0.05$, $**P < 0.01$, or $***P < 0.001$, with n.s. denoting non-significant $P \geq 0.05$.

Data availability

All data supporting the findings of this study are available within the article or from the corresponding author upon reasonable request (I. Sadowski, ijs.ubc@gmail.com).

537 **Acknowledgments**

538 We thank the laboratory staff at the BC Centre for Excellence in HIV/AIDS for processing
539 PBMCs from study participants. This research was supported by program project grant F16-
540 01210, from the Canadian Institutes of Health Research (CIHR), and F19-05392 Discovery
541 Grant from the Natural Sciences and Engineering Research Council of Canada (NSERC) (to
542 I.S.). PBMC collection from participants with HIV-1 was supported by CIHR project grant PJT-
543 159625 (to ZLB). ZLB is supported by a Michael Smith Health Research BC Scholar Award.

544 **Author Contributions**

545 Experimental design was conceived by Horvath R. M who also performed all experiments.
546 Brumme Z.L. provided PBMC samples from individuals on ART. Horvath R. M., Z.L. Brumme
547 and Sadowski I. wrote the manuscript.

548 **Conflicts of Interest**

549 The authors declare no conflicts of interest.

550 **References**

551

552 1. Davey RT, Bhat N, Yoder C, Chun TW, Metcalf JA, Dewar R, Natarajan V, Lempicki RA,
553 Adelsberger JW, Miller KD, Kovacs JA, Polis MA, Walker RE, Falloon J, Masur H, Gee
554 D, Baseler M, Dimitrov DS, Fauci AS, Lane HC. 1999. HIV-1 and T cell dynamics after
555 interruption of highly active antiretroviral therapy (HAART) in patients with a history of
556 sustained viral suppression. 26. Proc Natl Acad Sci U S A 96:15109–15114.

557 2. Zhang L, Chung C, Hu BS, He T, Guo Y, Kim AJ, Skulsky E, Jin X, Hurley A, Ramratnam
558 B, Markowitz M, Ho DD. 2000. Genetic characterization of rebounding HIV-1 after
559 cessation of highly active antiretroviral therapy. 7. J Clin Invest 106:839–845.

560 3. Sadowski I, Hashemi FB. 2019. Strategies to eradicate HIV from infected patients:
561 elimination of latent provirus reservoirs. Cell Mol Life Sci https://doi.org/10.1007/s00018-
562 019-03156-8.

563 4. Kim Y, Anderson JL, Lewin SR. 2018. Getting the "Kill" into "Shock and Kill": Strategies
564 to Eliminate Latent HIV. Cell Host & Microbe 23:14–26.

565 5. Yeh Y-HJ, Ho Y-C. 2021. Shock-and-kill versus block-and-lock: Targeting the fluctuating
566 and heterogeneous HIV-1 gene expression. 16. Proc Natl Acad Sci U S A
567 118:e2103692118.

568 6. Ait-Ammar A, Kula A, Darcis G, Verdikt R, De Wit S, Gautier V, Mallon PWG, Marcello
569 A, Rohr O, Van Lint C. 2019. Current Status of Latency Reversing Agents Facing the
570 Heterogeneity of HIV-1 Cellular and Tissue Reservoirs. Front Microbiol 10:3060.

571 7. McMahon DK, Zheng L, Cyktor JC, Aga E, Macatangay BJ, Godfrey C, Para M, Mitsuyasu
572 RT, Hesselgesser J, Dragavon J, Dobrowolski C, Karn J, Acosta EP, Gandhi RT, Mellors
573 JW. 2021. A Phase 1/2 Randomized, Placebo-Controlled Trial of Romidespin in Persons
574 With HIV-1 on Suppressive Antiretroviral Therapy. 4. J Infect Dis 224:648–656.

575 8. Siliciano JD, Siliciano RF. 2021. Low Inducibility of Latent Human Immunodeficiency
576 Virus Type 1 Proviruses as a Major Barrier to Cure. 12 Suppl 2. J Infect Dis 223:13–21.

577 9. Gunst JD, Højen JF, Søgaard OS. 2020. Broadly neutralizing antibodies combined with
578 latency-reversing agents or immune modulators as strategy for HIV-1 remission. 5. Curr
579 Opin HIV AIDS 15:309–315.

580 10. Powell AB, Ren Y, Korom M, Saunders D, Hanley PJ, Goldstein H, Nixon DF, Bollard CM,
581 Lynch RM, Jones RB, Cruz CRY. 2020. Engineered Antigen-Specific T Cells Secreting
582 Broadly Neutralizing Antibodies: Combining Innate and Adaptive Immune Response
583 against HIV. Mol Ther Methods Clin Dev 19:78–88.

584 11. Moranguinho I, Valente ST. 2020. Block-And-Lock: New Horizons for a Cure for HIV-1.
585 Viruses 12:1443.

586 12. Vansant G, Bruggemans A, Janssens J, Debyser Z. 2020. Block-And-Lock Strategies to Cure
587 HIV Infection. Viruses 12:84.

588 13. Lewis CA, Margolis DM, Browne EP. 2023. New Concepts in Therapeutic Manipulation of
589 HIV-1 Transcription and Latency: Latency Reversal versus Latency Prevention. Viruses
590 15:1677.

591 14. Parua PK, Fisher RP. 2020. Dissecting the Pol II transcription cycle and derailing cancer
592 with CDK inhibitors. Nat Chem Biol 16:716–724.

593 15. Zabihi M, Lotfi R, Yousefi A-M, Bashash D. 2023. Cyclins and cyclin-dependent kinases:
594 from biology to tumorigenesis and therapeutic opportunities. J Cancer Res Clin Oncol
595 149:1585–1606.

596 16. Buratowski S. 2009. Progression through the RNA Polymerase II CTD Cycle. Molecular
597 Cell 36:541–546.

598 17. Rodríguez-Molina JB, Tseng SC, Simonett SP, Taunton J, Ansari AZ. 2016. Engineered
599 Covalent Inactivation of TFIIH-Kinase Reveals an Elongation Checkpoint and Results in
600 Widespread mRNA Stabilization. 3. Mol Cell 63:433–444.

601 18. Rice AP. 2019. Roles of CDKs in RNA polymerase II transcription of the HIV-1 genome.
602 Transcription 10:111–117.

603 19. Kim YK, Bourgeois CF, Pearson R, Tyagi M, West MJ, Wong J, Wu S-Y, Chiang C-M,
604 Karn J. 2006. Recruitment of TFIIH to the HIV LTR is a rate-limiting step in the
605 emergence of HIV from latency. EMBO J 25:3596–3604.

606 20. Harper JW, Elledge SJ. 1998. The role of Cdk7 in CAK function, a retro-retrospective.
607 Genes & Development 12:285–289.

608 21. Malumbres M. 2014. Cyclin-dependent kinases 10.

609 22. Das AT, Harwig A, Berkhout B. 2011. The HIV-1 Tat Protein Has a Versatile Role in
610 Activating Viral Transcription. Journal of Virology 85:9506–9516.

611 23. Bartkowiak B, Liu P, Phatnani HP, Fuda NJ, Cooper JJ, Price DH, Adelman K, Lis JT,
612 Greenleaf AL. 2010. CDK12 is a transcription elongation-associated CTD kinase, the
613 metazoan ortholog of yeast Ctk1. 20. Genes Dev 24:2303–2316.

614 24. Blazek D, Kohoutek J, Bartholomeeusen K, Johansen E, Hulinkova P, Luo Z, Cimermancic
615 P, Ule J, Peterlin BM. 2011. The Cyclin K/Cdk12 complex maintains genomic stability via
616 regulation of expression of DNA damage response genes. 20. Genes Dev 25:2158–2172.

617 25. Ott M, Geyer M, Zhou Q. 2011. The Control of HIV Transcription: Keeping RNA
618 Polymerase II on Track. Cell Host & Microbe 10:426–435.

619 26. Core L, Adelman K. 2019. Promoter-proximal pausing of RNA polymerase II: a nexus of
620 gene regulation. 15–16. Genes Dev 33:960–982.

621 27. Chen FX, Smith ER, Shilatifard A. 2018. Born to run: control of transcription elongation by
622 RNA polymerase II. Nat Rev Mol Cell Biol 19:464–478.

623 28. Dollinger R, Gilmour DS. 2021. Regulation of Promoter Proximal Pausing of RNA
624 Polymerase II in Metazoans. Journal of Molecular Biology 433:166897.

625 29. Horvath RM, Brumme ZL, Sadowski I. 2023. Inhibition of the TRIM24 bromodomain
626 reactivates latent HIV-1. Sci Rep 13:556.

627 30. Horvath RM, Dahabieh M, Malcolm T, Sadowski I. 2023. TRIM24 controls induction of
628 latent HIV-1 by stimulating transcriptional elongation. Commun Biol 6:86.

629 31. Wang D, de la Fuente C, Deng L, Wang L, Zilberman I, Eadie C, Healey M, Stein D, Denny
630 T, Harrison LE, Meijer L, Kashanchi F. 2001. Inhibition of human immunodeficiency virus

631 type 1 transcription by chemical cyclin-dependent kinase inhibitors. 16. J Virol 75:7266–
632 7279.

633 32. Schang LM, Bantly A, Knockaert M, Shaheen F, Meijer L, Malim MH, Gray NS, Schaffer
634 PA. 2002. Pharmacological cyclin-dependent kinase inhibitors inhibit replication of wild-
635 type and drug-resistant strains of herpes simplex virus and human immunodeficiency virus
636 type 1 by targeting cellular, not viral, proteins. 15. J Virol 76:7874–7882.

637 33. Schonhofer C, Yi J, Sciorillo A, Andrae-Marobela K, Cochrane A, Harris M, Brumme ZL,
638 Brockman MA, Mounzer K, Hart C, Gyampoh K, Yuan Z, Montaner LJ, Tietjen I. 2021.
639 Flavonoid-based inhibition of cyclin-dependent kinase 9 without concomitant inhibition of
640 histone deacetylases durably reinforces HIV latency. Biochemical Pharmacology
641 186:114462.

642 34. Meijer L, Borgne A, Mulner O, Chong JP, Blow JJ, Inagaki N, Inagaki M, Delcros JG,
643 Moulinoux JP. 1997. Biochemical and cellular effects of roscovitine, a potent and selective
644 inhibitor of the cyclin-dependent kinases cdc2, cdk2 and cdk5. 1–2. Eur J Biochem
645 243:527–536.

646 35. Blagosklonny MV. 2004. Flavopiridol, an inhibitor of transcription: implications, problems
647 and solutions. 12. Cell Cycle 3:1537–1542.

648 36. Chao SH, Price DH. 2001. Flavopiridol inactivates P-TEFb and blocks most RNA
649 polymerase II transcription in vivo. 34. J Biol Chem 276:31793–31799.

650 37. Chen M, Li J, Zhang L, Wang L, Cheng C, Ji H, Altilia S, Ding X, Cai G, Altomare D,
651 Shtutman M, Byrum SD, Mackintosh SG, Feoktistov A, Soshnikova N, Mogila VA,

652 Tatarskiy V, Erokhin M, Chetverina D, Prawira A, Ni Y, Urban S, McInnes C, Broude EV,
653 Roninson IB. 2023. CDK8 and CDK19: positive regulators of signal-induced transcription
654 and negative regulators of Mediator complex proteins. Nucleic Acids Research gkad538.

655 38. Dannappel MV, Sooraj D, Loh JJ, Firestein R. 2019. Molecular and in vivo Functions of the
656 CDK8 and CDK19 Kinase Modules. Front Cell Dev Biol 6:171.

657 39. Constantin TA, Greenland KK, Varela-Carver A, Bevan CL. 2022. Transcription associated
658 cyclin-dependent kinases as therapeutic targets for prostate cancer. Oncogene 41:3303–
659 3315.

660 40. Luyties O, Taatjes DJ. 2022. The Mediator kinase module: an interface between cell
661 signaling and transcription. Trends in Biochemical Sciences S0968000422000056.

662 41. Horvath R, Brumme ZL, Sadowski I. 2023. CDK8 inhibitors antagonize HIV-1 reactivation
663 and promote provirus latency in T cells. preprint. Microbiology.

664 42. Chen M, Liang J, Ji H, Yang Z, Altilia S, Hu B, Schronce A, McDermott MSJ, Schools GP,
665 Lim C, Oliver D, Shtutman MS, Lu T, Stark GR, Porter DC, Broude EV, Roninson IB.
666 2017. CDK8/19 Mediator kinases potentiate induction of transcription by NFκB. Proc Natl
667 Acad Sci USA 114:10208–10213.

668 43. Firestein R, Bass AJ, Kim SY, Dunn IF, Silver SJ, Guney I, Freed E, Ligon AH, Vena N,
669 Ogino S, Chheda MG, Tamayo P, Finn S, Shrestha Y, Boehm JS, Jain S, Bojarski E,
670 Mermel C, Barretina J, Chan JA, Baselga J, Tabernero J, Root DE, Fuchs CS, Loda M,
671 Shivdasani RA, Meyerson M, Hahn WC. 2008. CDK8 is a colorectal cancer oncogene that
672 regulates β-catenin activity. Nature 455:547–551.

673 44. Bancerek J, Poss ZC, Steinparzer I, Sedlyarov V, Pfaffenwimmer T, Mikulic I, Dölken L,
674 Strobl B, Müller M, Taatjes DJ, Kovarik P. 2013. CDK8 Kinase Phosphorylates
675 Transcription Factor STAT1 to Selectively Regulate the Interferon Response. Immunity
676 38:250–262.

677 45. Budhiraja S, Famiglietti M, Bosque A, Planelles V, Rice AP. 2013. Cyclin T1 and CDK9 T-
678 Loop Phosphorylation Are Downregulated during Establishment of HIV-1 Latency in
679 Primary Resting Memory CD4+ T Cells. Journal of Virology 87:1211–1220.

680 46. Mbonye U, Wang B, Gokulrangan G, Shi W, Yang S, Karn J. 2018. Cyclin-dependent kinase
681 7 (CDK7)-mediated phosphorylation of the CDK9 activation loop promotes P-TEFb
682 assembly with Tat and proviral HIV reactivation. J Biol Chem 293:10009–10025.

683 47. Olson CM, Liang Y, Leggett A, Park WD, Li L, Mills CE, Elsarrag SZ, Ficarro SB, Zhang
684 T, Düster R, Geyer M, Sim T, Marto JA, Sorger PK, Westover KD, Lin CY, Kwiatkowski
685 N, Gray NS. 2019. Development of a Selective CDK7 Covalent Inhibitor Reveals
686 Predominant Cell-Cycle Phenotype. 6. Cell Chem Biol 26:792-803.e10.

687 48. Albert TK, Rigault C, Eickhoff J, Baumgart K, Antrecht C, Klebl B, Mittler G, Meisterernst
688 M. 2014. Characterization of molecular and cellular functions of the cyclin-dependent
689 kinase CDK9 using a novel specific inhibitor. 1. Br J Pharmacol 171:55–68.

690 49. Porter DC, Farmaki E, Altilia S, Schools GP, West DK, Chen M, Chang B-D, Puzyrev AT,
691 Lim C -u., Rokow-Kittell R, Friedhoff LT, Papavassiliou AG, Kalurupalle S, Hurteau G,
692 Shi J, Baran PS, Gyorffy B, Wentland MP, Broude EV, Kiaris H, Roninson IB. 2012.

693 Cyclin-dependent kinase 8 mediates chemotherapy-induced tumor-promoting paracrine
694 activities. Proceedings of the National Academy of Sciences 109:13799–13804.

695 50. Jordan A. 2003. HIV reproducibly establishes a latent infection after acute infection of T
696 cells in vitro. The EMBO Journal 22:1868–1877.

697 51. Hashemi FB, Barreto K, Bernhard W, Hashemi P, Lomness A, Sadowski I. 2016. HIV
698 Provirus Stably Reproduces Parental Latent and Induced Transcription Phenotypes
699 Regardless of the Chromosomal Integration Site. J Virol 90:5302–5314.

700 52. Laird GM, Bullen CK, Rosenbloom DIS, Martin AR, Hill AL, Durand CM, Siliciano JD,
701 Siliciano RF. 2015. Ex vivo analysis identifies effective HIV-1 latency–reversing drug
702 combinations. J Clin Invest 125:1901–1912.

703 53. Liu Q, Yin X, Languino LR, Altieri DC. 2018. Evaluation of Drug Combination Effect
704 Using a Bliss Independence Dose–Response Surface Model. Statistics in Biopharmaceutical
705 Research 10:112–122.

706 54. Bliss CI. 1939. THE TOXICITY OF POISONS APPLIED JOINTLY1. Annals of Applied
707 Biology 26:585–615.

708 55. Sadowski I, Mitchell DA. 2005. TFII-I and USF (RBF-2) regulate Ras/MAPK-responsive
709 HIV-1 transcription in T cells. European Journal of Cancer 41:2528–2536.

710 56. Kedei N, Lundberg DJ, Toth A, Welburn P, Garfield SH, Blumberg PM. 2004.
711 Characterization of the Interaction of Ingenol 3-Angelate with Protein Kinase C. Cancer
712 Research 64:3243–3255.

713 57. Li Z, Guo J, Wu Y, Zhou Q. 2013. The BET bromodomain inhibitor JQ1 activates HIV
714 latency through antagonizing Brd4 inhibition of Tat-transactivation. Nucleic Acids
715 Research 41:277–287.

716 58. Contreras X, Schweneker M, Chen C-S, McCune JM, Deeks SG, Martin J, Peterlin BM.
717 2009. Suberoylanilide hydroxamic acid reactivates HIV from latently infected cells. 11. J
718 Biol Chem 284:6782–6789.

719 59. Desimio MG, Giuliani E, Doria M. 2017. The histone deacetylase inhibitor SAHA
720 simultaneously reactivates HIV-1 from latency and up-regulates NKG2D ligands
721 sensitizing for natural killer cell cytotoxicity. Virology 510:9–21.

722 60. Jordan A. 2001. The site of HIV-1 integration in the human genome determines basal
723 transcriptional activity and response to Tat transactivation. The EMBO Journal 20:1726–
724 1738.

725 61. Brockman MA, Tanzi GO, Walker BD, Allen TM. 2006. Use of a novel GFP reporter cell
726 line to examine replication capacity of CXCR4- and CCR5-tropic HIV-1 by flow
727 cytometry. Journal of Virological Methods 131:134–142.

728 62. Weinberger LS, Burnett JC, Toettcher JE, Arkin AP, Schaffer DV. 2005. Stochastic Gene
729 Expression in a Lentiviral Positive-Feedback Loop: HIV-1 Tat Fluctuations Drive
730 Phenotypic Diversity. Cell 122:169–182.

731 63. Hansen MMK, Martin B, Weinberger LS. 2019. HIV Latency: Stochastic across Multiple
732 Scales. Cell Host & Microbe 26:703–705.

733 64. Larochelle S, Pandur J, Fisher RP, Salz HK, Suter B. 1998. Cdk7 is essential for mitosis and
734 for in vivo Cdk-activating kinase activity. Genes & Development 12:370–381.

735 65. Dahabieh MS, Ooms M, Brumme C, Taylor J, Harrigan PR, Simon V, Sadowski I. 2014.
736 Direct non-productive HIV-1 infection in a T-cell line is driven by cellular activation state
737 and NFκB. Retrovirology 11:17.

738 66. Dahabieh MS, Ooms M, Simon V, Sadowski I. 2013. A Doubly Fluorescent HIV-1 Reporter
739 Shows that the Majority of Integrated HIV-1 Is Latent Shortly after Infection. Journal of
740 Virology 87:4716–4727.

741 67. Battivelli E, Verdin E. 2018. HIVGKO: A Tool to Assess HIV-1 Latency Reversal Agents in
742 Human Primary CD4+ T Cells. BIO-PROTOCOL 8.

743 68. Hashemi P, Sadowski I. 2019. Diversity of small molecule HIV-1 latency reversing agents
744 identified in low- and high-throughput small molecule screens. Med Res Rev med.21638.

745 69. Cummins NW, Sainski AM, Dai H, Natesampillai S, Pang Y-P, Bren GD, de Araujo Correia
746 MCM, Sampath R, Rizza SA, O'Brien D, Yao JD, Kaufmann SH, Badley AD. 2016. Prime,
747 Shock, and Kill: Priming CD4 T Cells from HIV Patients with a BCL-2 Antagonist before
748 HIV Reactivation Reduces HIV Reservoir Size. J Virol 90:4032–4048.

749 70. Walker-Sperling VE, Pohlmeyer CW, Tarwater PM, Blankson JN. 2016. The Effect of
750 Latency Reversal Agents on Primary CD8 + T Cells: Implications for Shock and Kill
751 Strategies for Human Immunodeficiency Virus Eradication. EBioMedicine 8:217–229.

752 71. Abner E, Jordan A. 2019. HIV "shock and kill" therapy: In need of revision. Antiviral
753 Research 166:19–34.

754 72. Mousseau G, Kessing CF, Fromentin R, Trautmann L, Chomont N, Valente ST. 2015. The
755 Tat Inhibitor Didehydro-Cortistatin A Prevents HIV-1 Reactivation from Latency. mBio
756 6:e00465-15.

757 73. Kessing CF, Nixon CC, Li C, Tsai P, Takata H, Mousseau G, Ho PT, Honeycutt JB, Fallahi
758 M, Trautmann L, Garcia JV, Valente ST. 2017. In Vivo Suppression of HIV Rebound by
759 Didehydro-Cortistatin A, a "Block-and-Lock" Strategy for HIV-1 Treatment. Cell Reports
760 21:600–611.

761 74. Mori L, Jenike K, Yeh Y-HJ, Lacombe B, Li C, Getzler A, Mediouni S, Cameron M, Pipkin
762 M, Ho Y-C, Ramirez BC, Valente S. 2021. The XPB Subunit of the TFIIH Complex Plays
763 a Critical Role in HIV-1 Transcription and XPB Inhibition by Spironolactone Prevents
764 HIV-1 Reactivation from Latency. 4. J Virol 95:e01247-20, JVI.01247-20.

765 75. Yan C, Dodd T, He Y, Tainer JA, Tsutakawa SE, Ivanov I. 2019. Transcription preinitiation
766 complex structure and dynamics provide insight into genetic diseases. 6. Nat Struct Mol
767 Biol 26:397–406.

768 76. Karn J. 2011. The molecular biology of HIV latency: breaking and restoring the Tat-
769 dependent transcriptional circuit: Current Opinion in HIV and AIDS 6:4–11.

770 77. Canduri F, Perez PC, Caceres RA, de Azevedo WF. 2008. CDK9 a potential target for drug
771 development. 3. Med Chem 4:210–218.

772 78. Ahlenstiel CL, Symonds G, Kent SJ, Kelleher AD. 2020. Block and Lock HIV Cure
773 Strategies to Control the Latent Reservoir. Front Cell Infect Microbiol 10:424.

774 79. Biglione S, Byers SA, Price JP, Nguyen VT, Bensaude O, Price DH, Maury W. 2007.
775 Inhibition of HIV-1 replication by P-TEFb inhibitors DRB, seliciclib and flavopiridol
776 correlates with release of free P-TEFb from the large, inactive form of the complex.
777 Retrovirology 4:47.

778 80. Li J, Chen C, Ma X, Geng G, Liu B, Zhang Y, Zhang S, Zhong F, Liu C, Yin Y, Cai W,
779 Zhang H. 2016. Long noncoding RNA NRON contributes to HIV-1 latency by specifically
780 inducing tat protein degradation. Nat Commun 7:11730.

781 81. Jin H, Li D, Sivakumaran H, Lor M, Rustanti L, Cloonan N, Wani S, Harrich D. 2016.
782 Shutdown of HIV-1 Transcription in T Cells by Nullbasic, a Mutant Tat Protein. mBio
783 7:e00518-16, /mbio/7/4/e00518-16.atom.

784 82. Jin H, Sun Y, Li D, Lin M-H, Lor M, Rustanti L, Harrich D. 2019. Strong In Vivo Inhibition
785 of HIV-1 Replication by Nullbasic, a Tat Mutant. 4. mBio 10:e01769-19.

786

787

788

789 **Legends to Figures**

790

791 **Figure 1. Chemical inhibition of tCDKs is tolerated in T cells. A-C:** Molecular structure of
792 YKL-5-124 (CDK7 inhibitor) (**A**), LDC000067 (CDK9 inhibitor) (**B**), and Senexin A (CDK8
793 and CDK19 inhibitor) (**C**). **D:** Jurkat human T cells were treated with the concentrations of CDK
794 inhibitor for 24 hours after which cellular viability was determined. Results are normalized to an
795 untreated control (n = 2, mean ± SD).

796

797 **Figure 2. HIV-1 provirus requires tCDK kinase activity for reactivation. A:** Representative
798 flow cytometry scatter plots of JLat10.6 cells that were pre-treated for 30 min with DMSO
799 (Vehicle), 100 nM YKL-5-124 (CDK7i), 1 μM LDC000067 (CDK9i), or 10 μM Senexin A
800 (CDK8/19i) and subsequently incubated with 5 nM PMA and 1 μM ionomycin for 20 hours. **B,**
801 **C:** Following 30 min pre-treatment with the indicated concentration of tCDK inhibitor, JLat10.6
802 cells were incubated with 5 nM PMA and 1 μM ionomycin. 20 hours later, flow cytometric
803 analysis was performed to measure HIV-1 expression as reported as the proportion of GFP
804 positive cells (**B**) and the GFP delta (Δ) Mean Fluorescence Intensity (MFI) (**C**) (n = 2, mean
805 ± SD). **D:** As in (**A**), but JLat9.2 cells were examined. **E, F:** As in B, C, but JLat9.2 cells were
806 examined (n = 2, mean ± SD).

807

808 **Figure 3. tCDK inhibitors synergistically inhibit HIV-1 transcription. A - C:** JLat10.6 cells
809 were pre-treated for 30 minutes with 100 nM YKL-5-124 (CDK7i) and the indicated
810 concentration of LDC000067 (CDK9i) (**A**) or Senexin A (CDK8/19i) (**B**), or were pre-treated 30

811 minutes with 1 μM LDC000067 and the indicated concentration of Senexin A (**C**). Subsequently,
812 cells were incubated with 5 nM PMA/ 1 μM ionomycin for 20 hours and subsequently analyzed
813 by flow cytometry (*n* = 2, mean ± SD). **D - F:** Calculation of synergy between the indicated
814 treatments in **A - C** using Bliss Independence Modeling. Data are presented as the difference
815 between the predicted and the observed fractional HIV-1 expression response to the given drug
816 combination (*n* = 2, mean ± SD). See Materials and Methods for details.

817

818 **Figure 4. tCDK kinase inhibitors antagonize the effect of latency reversing agents. A, B:**
819 JLat10.6 cells were pre-treated for 30 minutes with 100 nM YKL-5-124 (CDK7i), 1 μM
820 LDC000067 (CDK9i), 10 μM Senexin A (CDK8/19i), or a vehicle control (Ve, DMSO).
821 Subsequently, cells were incubated with10 μM JQ1, 20 μM IACS-9571, 5 nM PEP005, 5 nM
822 PEP005/ 20 μM IACS-9571, 5 nM PMA/ 1 μM ionomycin, 5 μM SAHA, or were left untreated.
823 Following 20 hours, GFP expression was measured by flow cytometry and reported as the
824 percent of GFP positive cells (**A**) and the Mean Fluorescence Intensity (MFI) of GFP (**B**) (*n* = 2,
825 mean ± SD).

826

827 **Figure 5. Requirement of Tat for regulation of HIV-1 expression by tCDKs. A:**
828 Representative flow cytometry scatter plots of JLatA72 Jurkat cells (-Tat), pre-treated for 30
829 minutes with a vehicle control (DMSO), 100 nM YKL-5-124 (CDK7i), 1 μM LDC000067
830 (CDK9i), or 50 μM Senexin A (CDK8/19i) and subsequently incubated with 5 nM PMA and 1
831 μM ionomycin for 20 hours. **B, C:** JLatA72 cells were left untreated or pre-treated for 30
832 minutes with a vehicle control (DMSO), 100 nM YKL-5-124, 1 μM LDC00067, or 50 μM

833 Senexin A prior to stimulation with 5 nM PMA/ 1 μM ionomycin. Following 20 hours, flow
834 cytometry was performed with viral expression reported as the percent of GFP positive cells (**B**)
835 and the delta GFP Mean Fluorescence Intensity (MFI) (**C**) (n = 2, mean ± SD).

836

837 **Figure 6. Effect of sustained tCDK inhibition on cell growth and viability. A, B:** Jurkat T
838 cells were incubated with the indicated concentration of YKL-5-124 or a vehicle control (Ve,
839 DMSO) for the indicated time (Days), total cell count (**A**) and viability (**B**) were determined.
840 Media was replaced daily with inhibitor (n = 3, mean ± SD). **C, D:** As in (**A**) and (**B**), but cells
841 were treated with LDC000067 (n = 3, mean ± SD). **E, F:** Performed as previously described but
842 Jurkat cells were incubated with the indicated concentration of Senexin A (n = 3, mean ± SD).

843

844 **Figure 7. Inhibition of tCDK activity encourages establishment of latency upon infection.**
845 **A:** Simplified depiction of the replication incompetent Red-Green-HIV-1 (RGH) dual reporter
846 virus (66), which expresses GFP from the 5' LTR and mCherry from an internal constitutive
847 PGK promoter. **B:** Jurkat $CD4^+$ human T cells were left untreated or were pre-treated for 30
848 minutes with 100 nM YKL-5-124, 1 μM LDC000067, or 10 μM Senexin A prior to infection of
849 cells with RGH. 1-day post-infection, media was replaced, and cells were either washed of the
850 drug or maintained with the same concentration of inhibitor. 4 days post-infection, proviral
851 expression was assessed by flow cytometry. **C:** Representative flow cytometry scatter plots of
852 RGH infected cells, treated as indicated in (**B**) and examined 4 days post-infection. **D:** Jurkat T
853 cells were treated as in (**B**), with the percentage of productive infections determined by flow
854 cytometry 4 days post-infection. The % Productive Infections was determined from the ratio of

855 GFP+/mCherry+ cells to all mCherry+ cells (*n* = 3, mean ± SD). **E:** Summary of the infection
856 rate for cells treated as indicated, representing the proportion of cells expressing mCherry
857 expression (*n* = 3, mean ± SD).

858

859 **Figure 8. Effect of CDK9 and CDK8/19 inhibitors on basal expression of an HIV-1 mini-**
860 **virus. A:** Schematic depiction of the mini-dual HIV-1 reporter virus in the mdHIV #77 Jurkat
861 Tat clonal T cell line (51), which expresses dsRed from the 5' LTR and eGFP from an internal
862 EF1α promoter. **B:** mdHIV #77 cells were incubated with a vehicle control (DMSO), 1 μM
863 LDC000067, 10 μM Senexin A, or 1 μM LDC000067 and 10 μM Senexin A for 14 days, when
864 the drug(s) were removed, and HIV-1 expression was assessed by flow cytometry over the
865 indicated time (Days). **C:** Representative flow cytometry scatter plots following 4 days of drug
866 treatment followed by 4 days after drug withdrawal. Each dot indicates a single HIV-1 infected
867 cell, where the population in Q2 represents cells with transcriptionally active provirus. **D:**
868 mdHIV #77 cells were treated as in (**B**) with viral expression assessed on the indicated day by
869 flow cytometry (*n* = 2, mean ± SD). **E:** mdHIV #77 cells treated as indicated in (**B**) were
870 examined for viability, with values normalized to the vehicle control (*n* = 2, mean ± SD).

871

872 **Figure 9. Effect of CDK9 and CDK8/19 inhibitors on RGH proviral latency. A:** Schematic
873 depiction of the full-length, replication incompetent HIV-1 RGH reporter virus chromosomally
874 integrated in the RGH #20 Jurkat clonal T cell line, where eGFP is expressed from the 5' LTR,
875 and mCherry from an internal PGK promoter that replaces *Nef*. **B:** RGH #20 cells were
876 incubated with a vehicle control (DMSO), 1 μM LDC000067, 10 μM Senexin A, or 1 μM

877 LDC000067 and 10 μM Senexin A for 7 days, when drug(s) were removed, and viral expression
878 was measured by flow cytometry for 10 more days. **C:** Representative flow cytometry scatter
879 plots following 4 days of drug treatment and 4 days following drug withdrawal. All "dots" are
880 indicative of a single HIV-1 infected cell with Q2 (eGFP+/mCherry+) displaying cells with
881 transcriptionally active provirus. **D:** RGH #20 cells were treated as in (**B**) with viral expression
882 assessed on the indicated day by flow cytometry (*n* = 2, mean ± SD). **E:** RGH #20 cells treated
883 as indicated in (**B**) were examined for viability, with values normalized to the vehicle control (*n*
884 = 2, mean ± SD).

885

886 **Figure 10. tCDK activity is required for reactivation of HIV-1 in CD4$^+$ PBMCs *ex vivo*. A -**
887 **C:** PBMCs isolated from HIV-1 infected individuals on ART, were left untreated or pre-treated
888 for 30 minutes with Vehicle (DMSO), 100 nM YKL-5-124, 1 μM LDC000067, 10 μM Senexin
889 A, or 1 μM LDC000067/ 10 μM Senexin A. Following pre-treatment, cells were incubated with
890 5nM PMA/ 1μM Ionomycin for 24 hours after which intracellular RNA was extracted and
891 analyzed using RT-PCR with oligos specific for multiply spliced Tat-Rev HIV-1 mRNA
892 transcripts. HIV-1 mRNA expression is normalized to *GAPDH* (*n* = 3 - 4, mean ± SD).

893

894

Table 1

Patient	ID	Sex	Intact HIV Copies/Million $CD4^+$ T cells	Total HIV Copies/Million $CD4^+$ T cells	%Intact
A	BC024	Male	339.88	4941.32	6.88
B	BC030	Male	397.27	3774.98	10.52
C	BC002	Male	197.31	4857.65	4.06

Figure 1

A

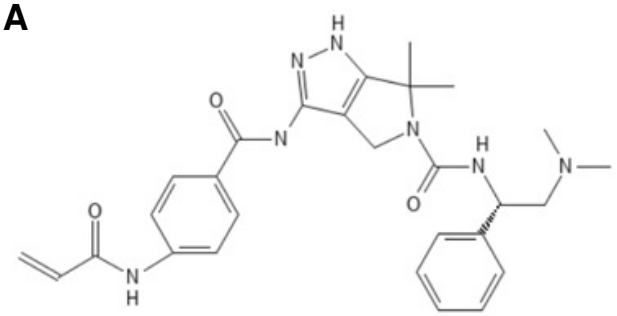

YKL-5-124 – CDK7 Inhibitor

B

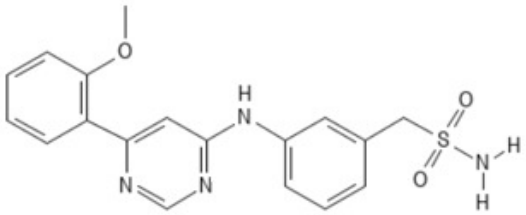

LDC000067 – CDK9 Inhibitor

C

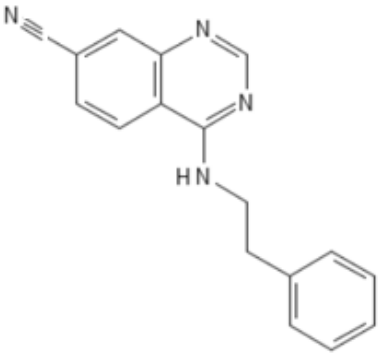

Senexin A – CDK8/19 Inhibitor

D

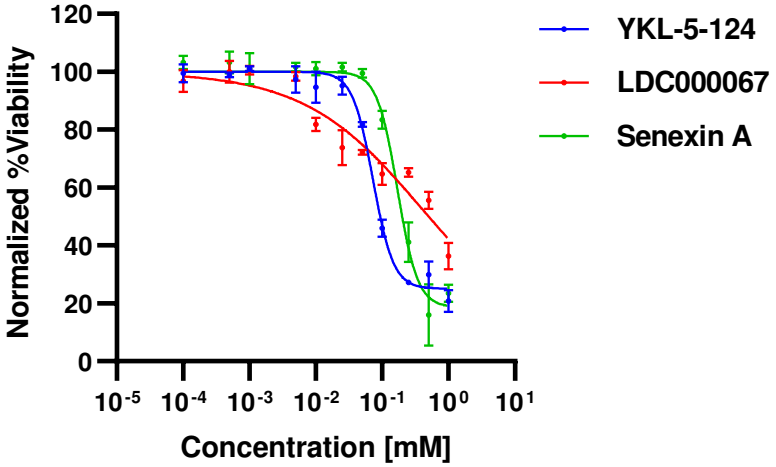

LC50: 93 µM, 499 µM, 200 µM

Figure 2

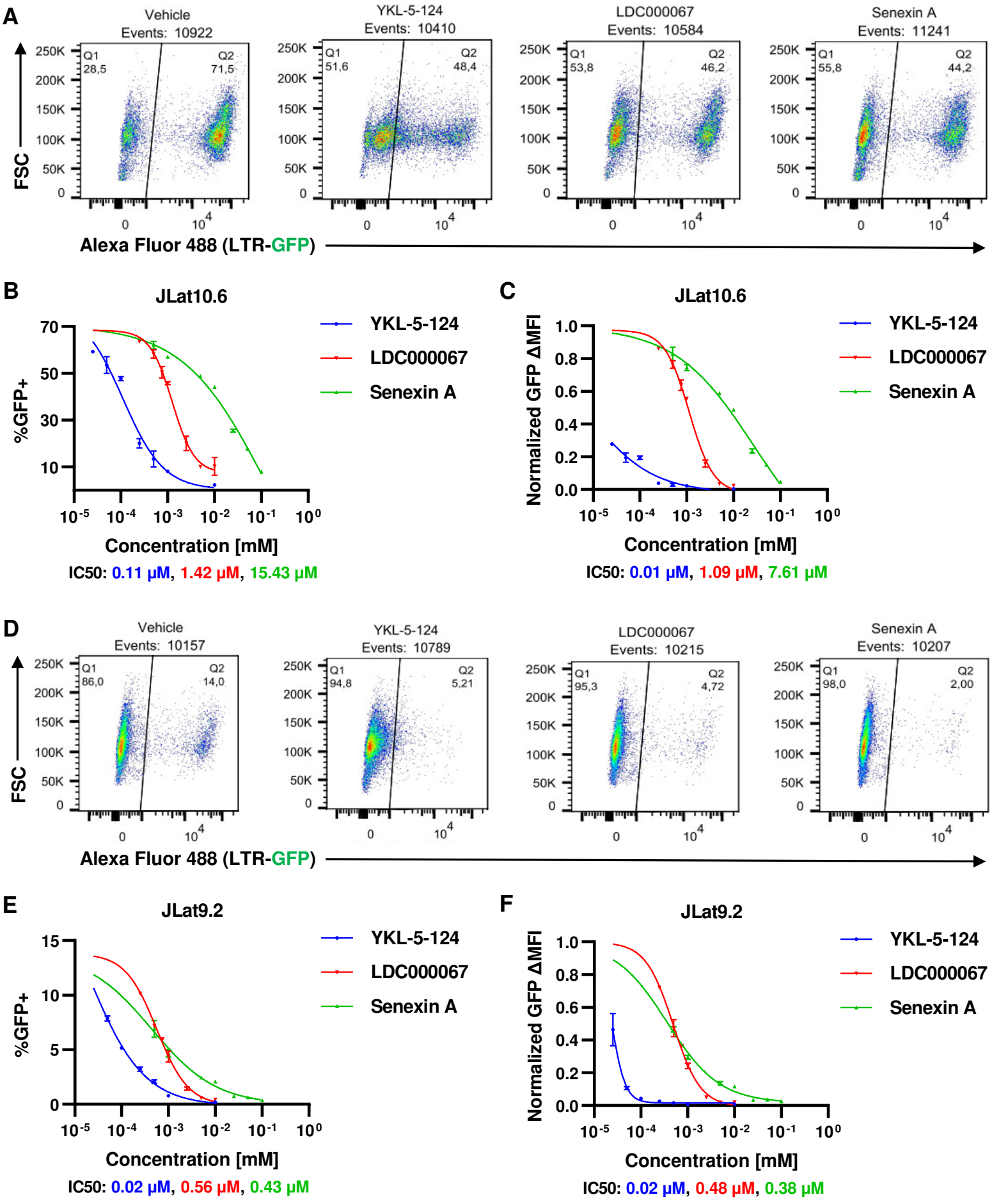
A
Vehicle
Events: 10922
Q1 28,5
Q2 71,5
YKL-5-124
Events: 10410
Q1 51,6
Q2 48,4
LDC000067
Events: 10584
Q1 53,8
Q2 46,2
Senexin A
Events: 11241
Q1 55,8
Q2 44,2
FSC
Alexa Fluor 488 (LTR-GFP)
B
JLat10.6
%GFP+
Concentration [mM]
YKL-5-124
LDC000067
Senexin A
IC50: 0.11 µM, 1.42 µM, 15.43 µM
C
JLat10.6
Normalized GFP ΔMFI
Concentration [mM]
YKL-5-124
LDC000067
Senexin A
IC50: 0.01 µM, 1.09 µM, 7.61 µM
D
Vehicle
Events: 10157
Q1 86,0
Q2 14,0
YKL-5-124
Events: 10789
Q1 94,8
Q2 5,21
LDC000067
Events: 10215
Q1 95,3
Q2 4,72
Senexin A
Events: 10207
Q1 98,0
Q2 2,00
FSC
Alexa Fluor 488 (LTR-GFP)
E
JLat9.2
%GFP+
Concentration [mM]
YKL-5-124
LDC000067
Senexin A
IC50: 0.02 µM, 0.56 µM, 0.43 µM
F
JLat9.2
Normalized GFP ΔMFI
Concentration [mM]
YKL-5-124
LDC000067
Senexin A
IC50: 0.02 µM, 0.48 µM, 0.38 µM

Figure 3

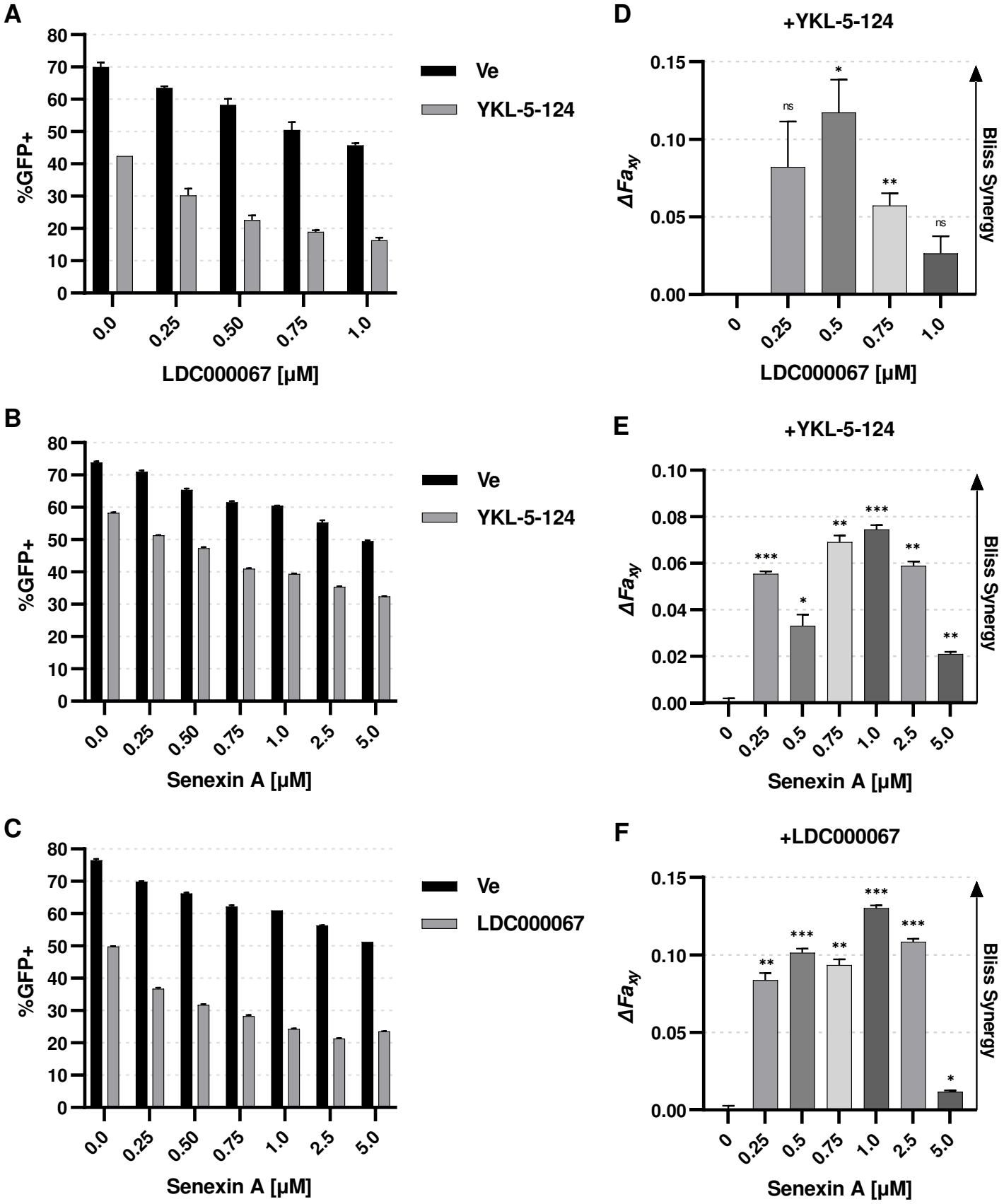
A
%GFP+
80
70
60
50
40
30
20
10
0
0.0
0.25
0.50
0.75
1.0
LDC000067 [μM]
Ve
YKL-5-124
B
%GFP+
0.0
0.25
0.50
0.75
1.0
2.5
5.0
Senexin A [μM]
Ve
YKL-5-124
C
%GFP+
Senexin A [μM]
Ve
LDC000067
D
+YKL-5-124
ΔFa_{xy}
0.15
0.10
0.05
0.00
ns
*
**
ns
0
0.25
0.5
0.75
1.0
LDC000067 [μM]
Bliss Synergy
E
+YKL-5-124
ΔFa_{xy}
0.10
0.08
0.06
0.04
0.02
0.00
***
*
**
***
**
**
0
0.25
0.5
0.75
1.0
2.5
5.0
Senexin A [μM]
Bliss Synergy
F
+LDC000067
ΔFa_{xy}
0.15
0.10
0.05
0.00
**
***
**
***
***
*
0
0.25
0.5
0.75
1.0
2.5
5.0
Senexin A [μM]
Bliss Synergy

Figure 4

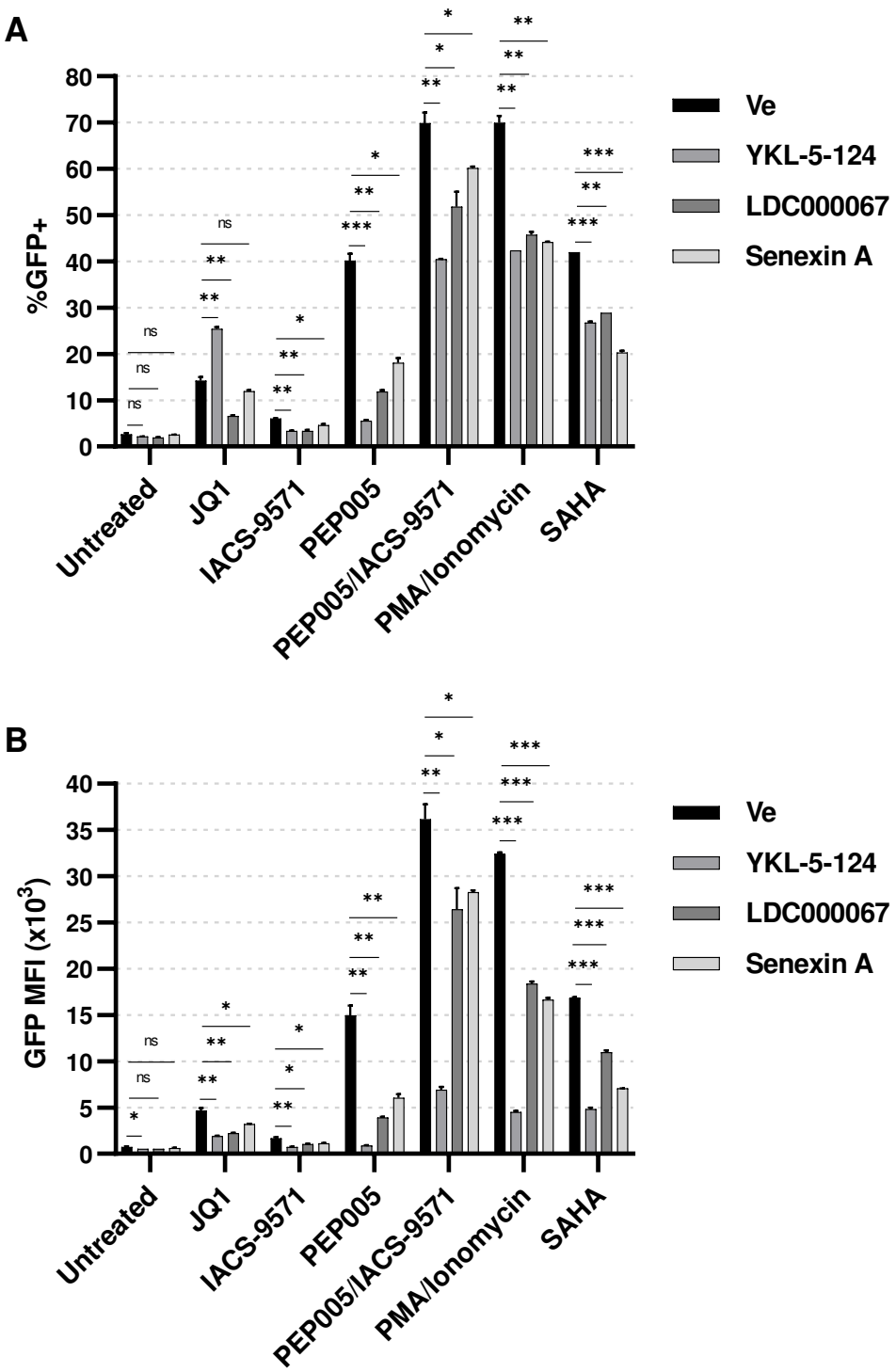
A
%GFP+
80
70
60
50
40
30
20
10
0
Untreated
JQ1
IACS-9571
PEP005
PEP005/IACS-9571
PMA/Ionomycin
SAHA
Ve
YKL-5-124
LDC000067
Senexin A
B
GFP MFI (x10^3)
40
35
30
25
20
15
10
5
0
Untreated
JQ1
IACS-9571
PEP005
PEP005/IACS-9571
PMA/Ionomycin
SAHA
Ve
YKL-5-124
LDC000067
Senexin A

Figure 5

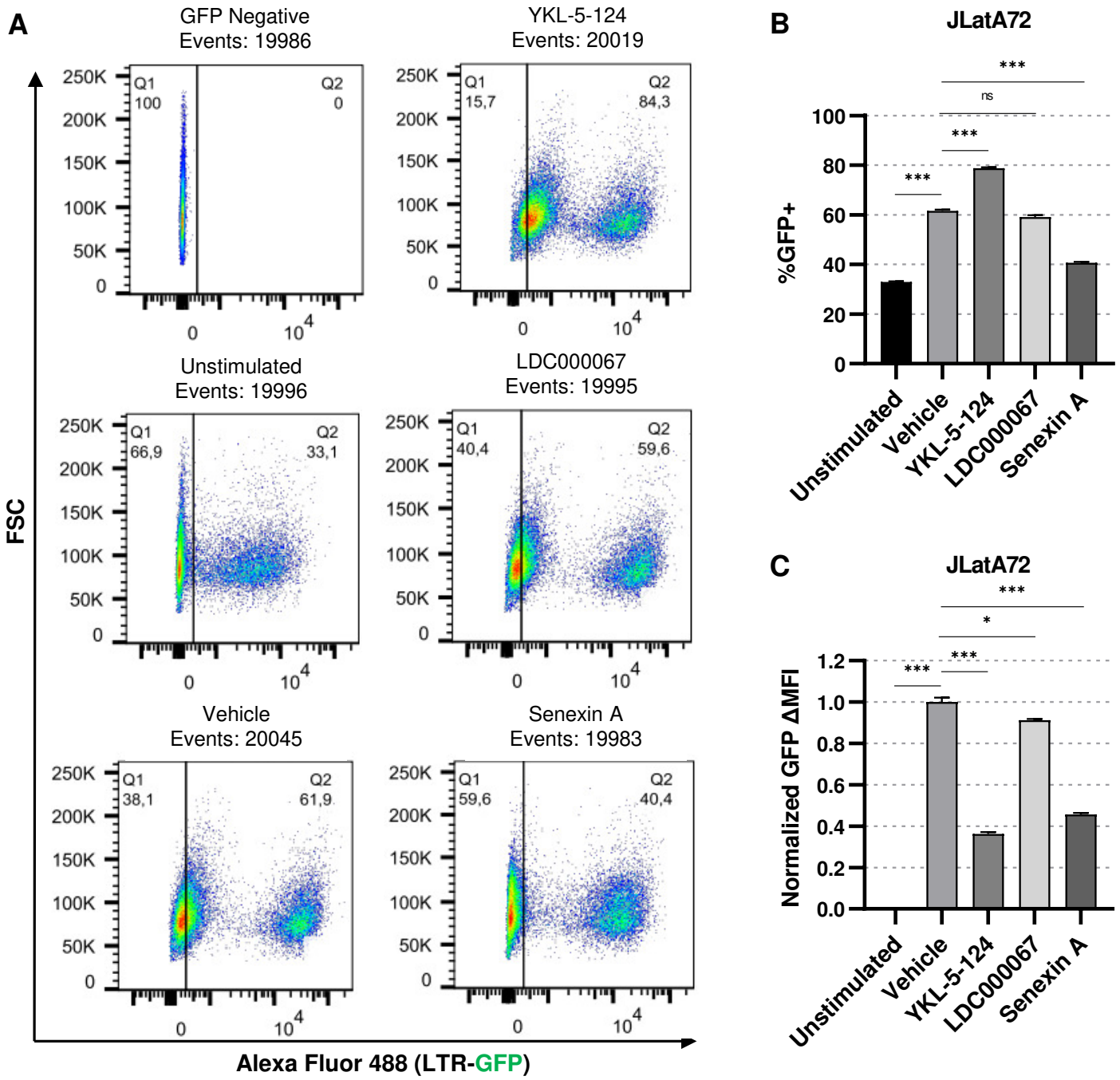
A
GFP Negative
Events: 19986
Q1
100
Q2
0
YKL-5-124
Events: 20019
Q1
15,7
Q2
84,3
Unstimulated
Events: 19996
Q1
66,9
Q2
33,1
LDC000067
Events: 19995
Q1
40,4
Q2
59,6
Vehicle
Events: 20045
Q1
38,1
Q2
61,9
Senexin A
Events: 19983
Q1
59,6
Q2
40,4
250K
200K
150K
100K
50K
0
10^4
FSC
Alexa Fluor 488 (LTR-GFP)
B
JLatA72
%GFP+
ns
***
Unstimulated
Vehicle
YKL-5-124
LDC000067
Senexin A
C
JLatA72
Normalized GFP ΔMFI
*

Figure 6

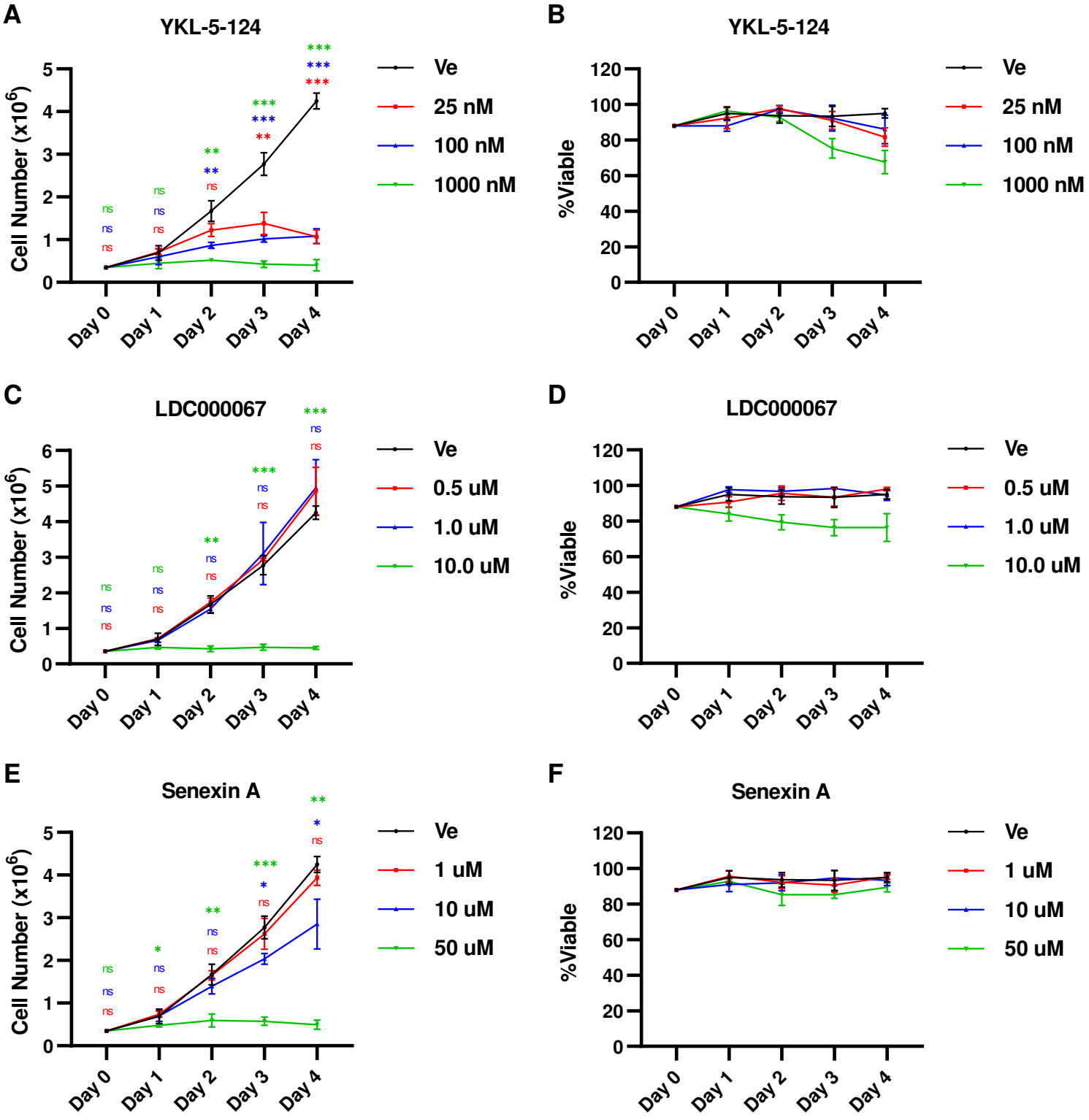
A
YKL-5-124
Cell Number (x10^6)
Day 0
Day 1
Day 2
Day 3
Day 4
Ve
25 nM
100 nM
1000 nM
B
YKL-5-124
%Viable
C
LDC000067
0.5 uM
1.0 uM
10.0 uM
D
E
Senexin A
1 uM
10 uM
50 uM
F

Figure 7

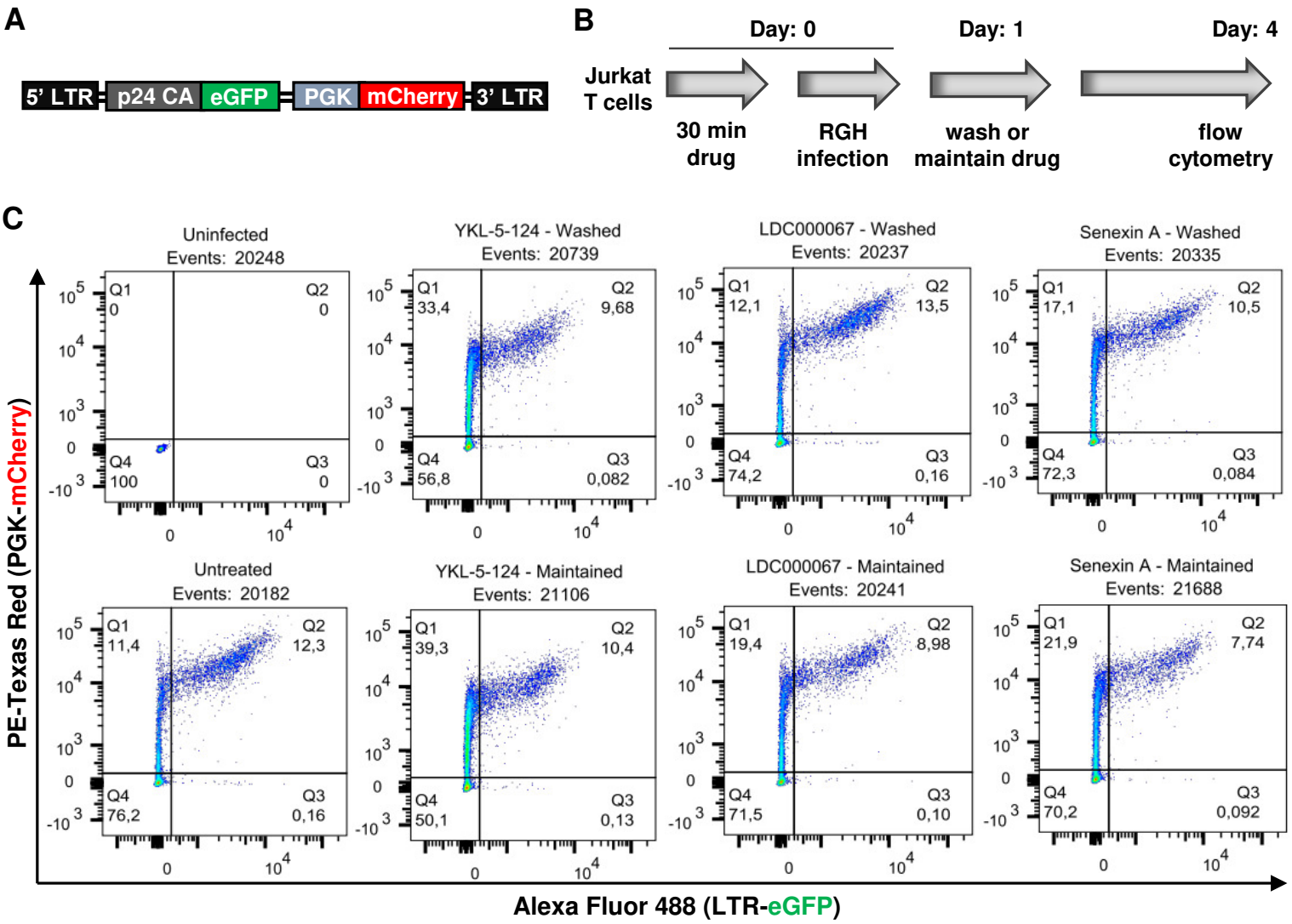
A
5' LTR
p24 CA
eGFP
PGK
mCherry
3' LTR
B
Day: 0
Day: 1
Day: 4
Jurkat T cells
30 min drug
RGH infection
wash or maintain drug
flow cytometry
C
Uninfected
Events: 20248
Q1 0
Q2 0
Q4 100
Q3 0
YKL-5-124 - Washed
Events: 20739
Q1 33,4
Q2 9,68
Q4 56,8
Q3 0,082
LDC000067 - Washed
Events: 20237
Q1 12,1
Q2 13,5
Q4 74,2
Q3 0,16
Senexin A - Washed
Events: 20335
Q1 17,1
Q2 10,5
Q4 72,3
Q3 0,084
Untreated
Events: 20182
Q1 11,4
Q2 12,3
Q4 76,2
Q3 0,16
YKL-5-124 - Maintained
Events: 21106
Q1 39,3
Q2 10,4
Q4 50,1
Q3 0,13
LDC000067 - Maintained
Events: 20241
Q1 19,4
Q2 8,98
Q4 71,5
Q3 0,10
Senexin A - Maintained
Events: 21688
Q1 21,9
Q2 7,74
Q4 70,2
Q3 0,092
PE-Texas Red (PGK-mCherry)
Alexa Fluor 488 (LTR-eGFP)
D
%Productive Infections
Untreated
YKL-5-124
LDC000067
Senexin A
Washed
Maintained
ns
***
E
%Infected Population
Ve
YKL-5-124
LDC000067
Senexin A

Figure 8

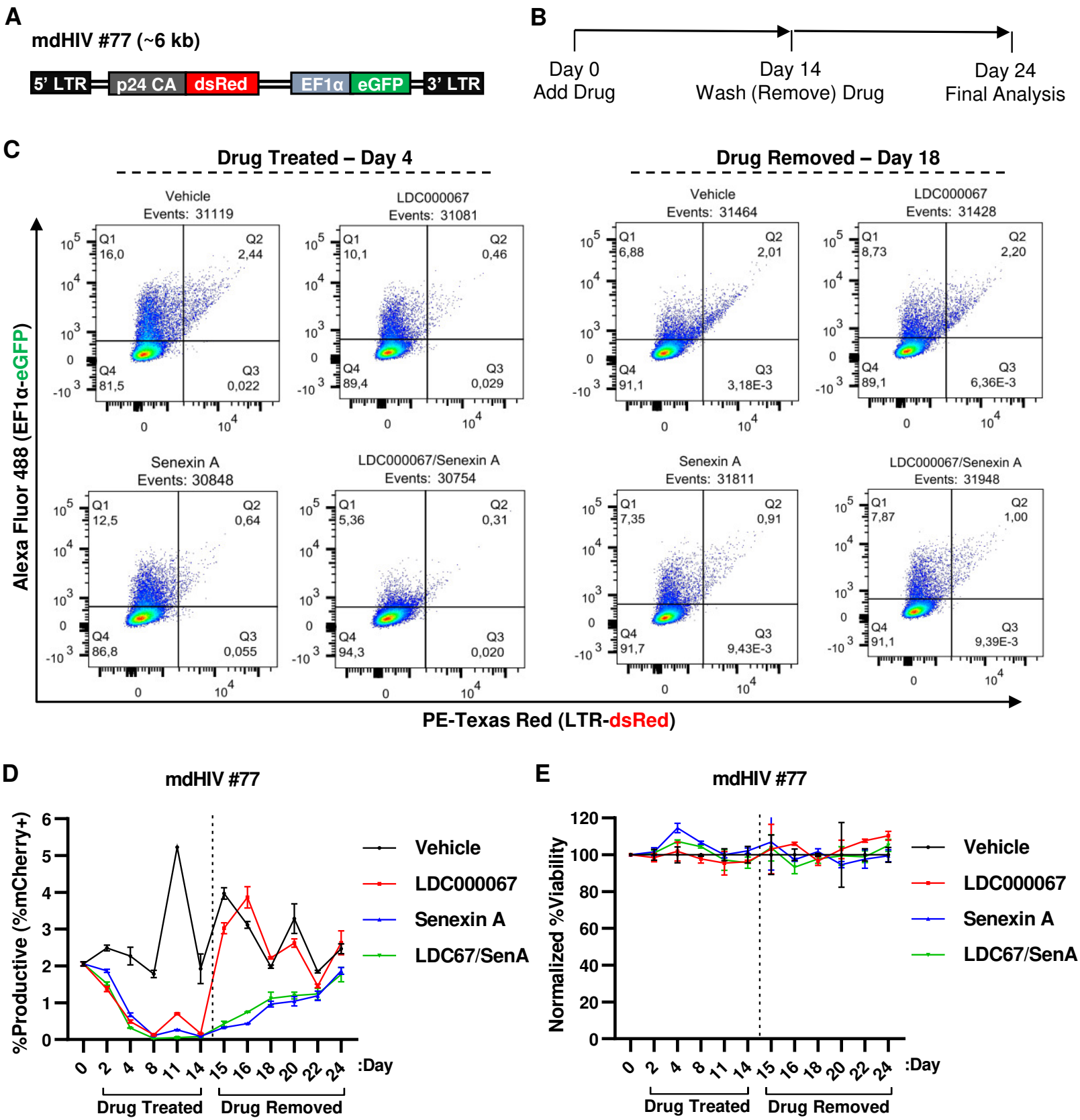
A
mdHIV #77 (~6 kb)
5' LTR
p24 CA
dsRed
EF1α
eGFP
3' LTR
B
Day 0
Add Drug
Day 14
Wash (Remove) Drug
Day 24
Final Analysis
C
Drug Treated – Day 4
Drug Removed – Day 18
Vehicle
Events: 31119
Q1 16,0
Q2 2,44
Q4 81,5
Q3 0,022
LDC000067
Events: 31081
Q1 10,1
Q2 0,46
Q4 89,4
Q3 0,029
Vehicle
Events: 31464
Q1 6,88
Q2 2,01
Q4 91,1
Q3 3,18E-3
LDC000067
Events: 31428
Q1 8,73
Q2 2,20
Q4 89,1
Q3 6,36E-3
Senexin A
Events: 30848
Q1 12,5
Q2 0,64
Q4 86,8
Q3 0,055
LDC000067/Senexin A
Events: 30754
Q1 5,36
Q2 0,31
Q4 94,3
Q3 0,020
Senexin A
Events: 31811
Q1 7,35
Q2 0,91
Q4 91,7
Q3 9,43E-3
LDC000067/Senexin A
Events: 31948
Q1 7,87
Q2 1,00
Q4 91,1
Q3 9,39E-3
Alexa Fluor 488 (EF1α-eGFP)
PE-Texas Red (LTR-dsRed)
D
mdHIV #77
%Productive (%mCherry+)
Vehicle
LDC000067
Senexin A
LDC67/SenA
:Day
Drug Treated
Drug Removed
E
mdHIV #77
Normalized %Viability
Vehicle
LDC000067
Senexin A
LDC67/SenA
:Day
Drug Treated
Drug Removed

Figure 9

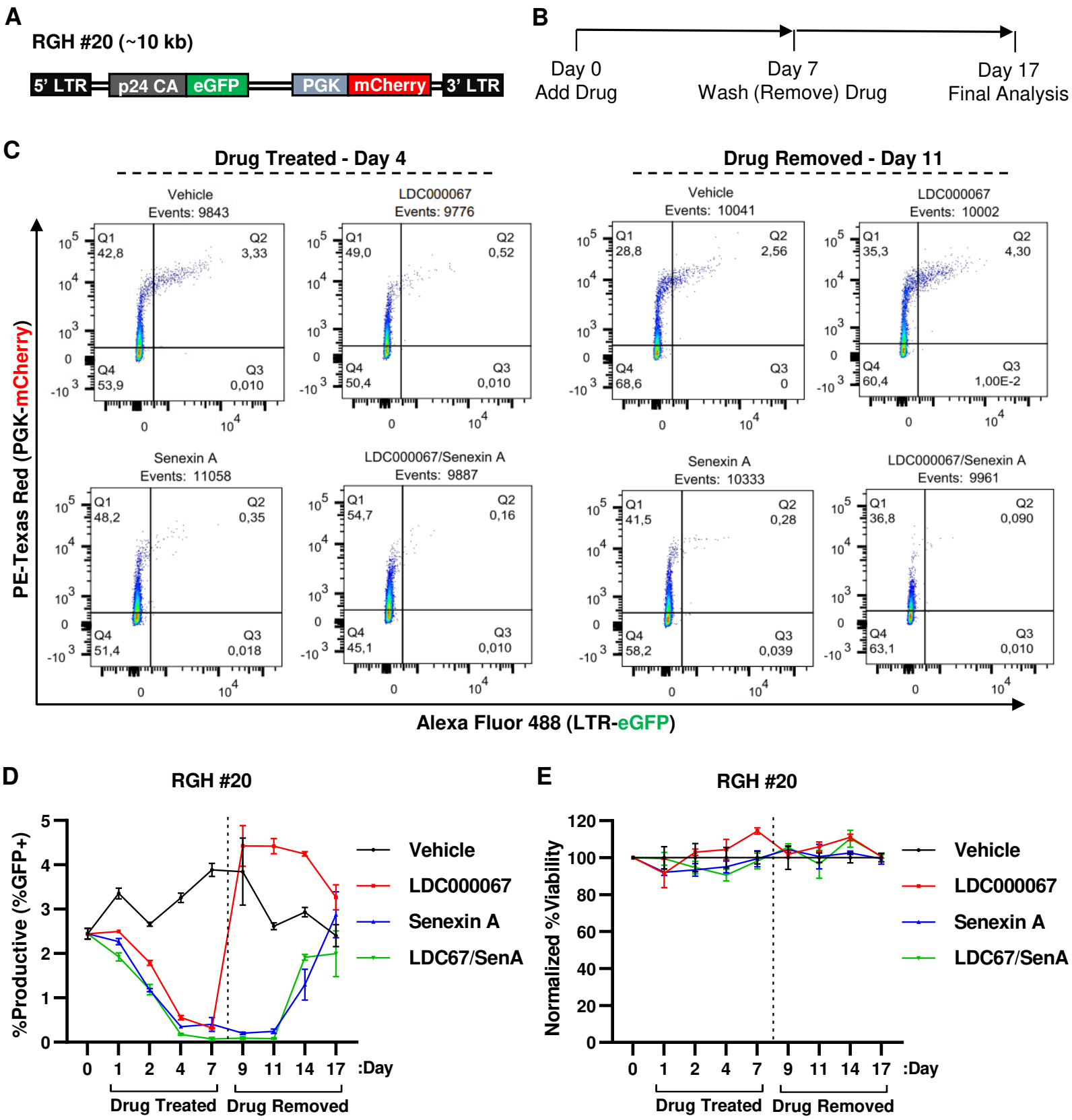
A
RGH #20 (~10 kb)
5' LTR
p24 CA
eGFP
PGK
mCherry
3' LTR
B
Day 0
Add Drug
Day 7
Wash (Remove) Drug
Day 17
Final Analysis
C
Drug Treated - Day 4
Drug Removed - Day 11
Vehicle
Events: 9843
Q1 42,8
Q2 3,33
Q4 53,9
Q3 0,010
LDC000067
Events: 9776
Q1 49,0
Q2 0,52
Q4 50,4
Q3 0,010
Vehicle
Events: 10041
Q1 28,8
Q2 2,56
Q4 68,6
Q3 0
LDC000067
Events: 10002
Q1 35,3
Q2 4,30
Q4 60,4
Q3 1,00E-2
Senexin A
Events: 11058
Q1 48,2
Q2 0,35
Q4 51,4
Q3 0,018
LDC000067/Senexin A
Events: 9887
Q1 54,7
Q2 0,16
Q4 45,1
Q3 0,010
Senexin A
Events: 10333
Q1 41,5
Q2 0,28
Q4 58,2
Q3 0,039
LDC000067/Senexin A
Events: 9961
Q1 36,8
Q2 0,090
Q4 63,1
Q3 0,010
PE-Texas Red (PGK-mCherry)
Alexa Fluor 488 (LTR-eGFP)
D
RGH #20
%Productive (%GFP+)
Vehicle
LDC000067
Senexin A
LDC67/SenA
:Day
Drug Treated
Drug Removed
E
RGH #20
Normalized %Viability
Vehicle
LDC000067
Senexin A
LDC67/SenA
:Day
Drug Treated
Drug Removed

Figure 10

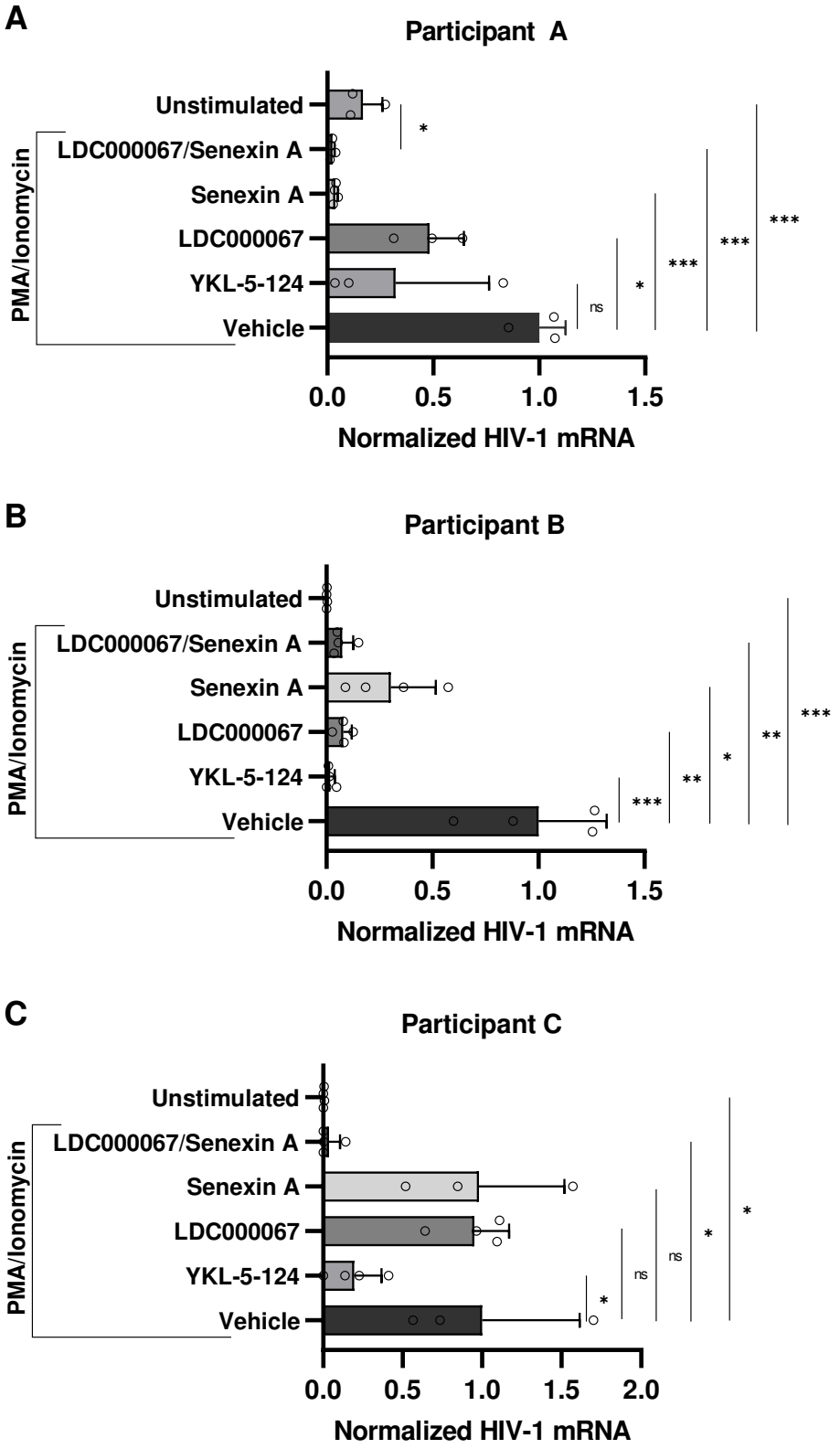
A
Participant A
Unstimulated
LDC000067/Senexin A
Senexin A
LDC000067
YKL-5-124
Vehicle
PMA/Ionomycin
*
ns
*
***
***
***
0.0
0.5
1.0
1.5
Normalized HIV-1 mRNA
B
Participant B
Unstimulated
LDC000067/Senexin A
Senexin A
LDC000067
YKL-5-124
Vehicle
PMA/Ionomycin
***
**
*
**
***
0.0
0.5
1.0
1.5
Normalized HIV-1 mRNA
C
Participant C
Unstimulated
LDC000067/Senexin A
Senexin A
LDC000067
YKL-5-124
Vehicle
PMA/Ionomycin
*
ns
ns
*
*
0.0
0.5
1.0
1.5
2.0
Normalized HIV-1 mRNA